Chapter 5

The Application of Surface Acoustic Waves in Surface Semiconductor Investigations and Gas Sensors

Marian Urbańczyk and Tadeusz Pustelny

Additional information is available at the end of the chapter

http://dx.doi.org/10.5772/53717

1. Introduction

An ever-growing interest in the physical properties of the semiconductor surface results both from the influence of processes occurring at the surface, on the properties of semiconductors, and from the influence of the physical surface structure on the operation of semiconductor devices. Among the methods of investigations of semiconductor surfaces, there are no methods of investigating the dynamic properties of electrical carries in fast and very fast energetic surface states [1-5]. Up to now the existing methods allow only to investigate the surface sates with a carrier life-time τ of above 10^{-6}s [6]. In the case of extrinsic semiconductors the surface states may, however, be considerably faster (the carrier life-time in surface traps is usually less than 10^{-8}s). In such cases the existing methods of determining the parameters of fast surface states allow only to estimate these parameters, since the obtained results exhibit a considerable uncertainty. Therefore investigations of the kinetic properties of fast surface states are not popular and there are no new results concerning their determination.

For some years attention has been paid to the influence of the physical state of the near-surface region of a semiconductor on the results of investigations of the acoustoelectric effects in piezoelectric-semiconductor systems. Recently also attention has been paid to the possibility of applying Rayleigh's acoustic surface waves in investigations of various parameters of solid states [7-9].

Theoretical and experimental investigations of the application of acoustoelectric effects for the determination of carrier properties in the near surface region (e.g. the electrical surface potential, carrier concentration, electrical conductivities,…) are being run all the time. Problems of the influences of chemical and mechanical surface treatments realized in the

first step of preparations of semiconductor plates (wafers) on kinetic and electron features of electrical carriers have not often been taken up. The quantitative data concerning the effective life-time τ and the velocity of carrier trapping g are presented very seldom. Results of investigations have shown that acoustic methods based on the acoustoelectric effects with using surface acoustic waves can be applied to determine the parameters of fast and very fast surface states in semiconductors. An analysis of the methods shows that the accuracy of the obtained surface parameters are standard about some presents, which is a rather good accuracy in the determination of the parameters of fast surface states. By means of acoustic methods both element-semiconductors and compound semiconductors can be investigated (among others – semiconductors of the III-V group).

There are many methods of gas detection and a comprehensive review can be found in literature [10-17]. Since the early MOS field transistors and Schottky diodes sensors through the first SAW devices made by D'Amico [18] we have now many different fiber optic hydrogen sensors [19,20]. For example, hydrogen gas is used as a reducing agent and as a carrier gas in the process of manufacturing semiconductors and it has been increasingly noted as a clean source of energy or a fuel gas. A leak of hydrogen in large quantities should be avoided because if mixed with air in a ratio of 4.65 - 93.9 vol. %, hydrogen is explosive. Thus a fast and precise detection of hydrogen near and especially before the explosive concentration and at room temperature is still a great problem. In nowadays very important problem is connected with detection extremely low concentration of explosives material.

Surface acoustic wave gas sensors are especially attractive because of their remarkable sensitivities due to changes of the boundary conditions for propagating acoustic Rayleigh waves, introduced by the interaction of a thin active sensor layer with specific gas molecules. This unusual sensitivity results from the simple fact that most of the wave energy is concentrated near the crystal surface within one or two wavelengths. Consequently, the surface wave is in its first approximation highly sensitive to changes of the physical or chemical properties of the thin active sensor layer placed on the surface of the piezoelectric delay line. As long as the whole thickness of the sensor material is much smaller than the surface wave wavelength one can speak of a perturbation of the Rayleigh wave [21, 22]. Otherwise, we have to take into account other types of waves, such as Love waves, which can propagate in layered structures [23].

A very interesting feature of SAW sensors is the fact that the layered sensor structure on a piezoelectric substrate provides new possibilities of detecting gas in a SAW sensor system by using the acoustoelectric coupling between the surface wave and the free charges in a semiconductor sensor layer [24]. For selective detection gas particles must be used with specific chemical sensor layers placed on the piezoelectric acoustic line. Any change in the physical properties of this sensor layer results from changes of gas atmosphere, varies the conditions of acoustic wave propagation. Therefore, the propagation velocity and attenuation of the acoustic wave are changed, too. Mass and electrical effects, such as perturbations in mechanical and electrical boundary conditions, will be considered separately. Perturbations of the mechanical boundary conditions are important in a sensor with a dielectric sensor layer. Perturbations in electrical boundary conditions are important

in a sensor with a conducting or semiconducting sensor layer. These two effects occur simultaneously in the interaction time of an active film with a specific gas and are additive because of their small values. For instance, in thin phtalocyanine films as organic semiconductors both of these exist, but the electric effect is much greater (several times, depending on the gas concentration) [25].

For sensor construction and optimization conditions of working it is important to get an analytic model of the SAW sensor. Here we provide theoretical information concerning the acoustoelectric effect in the piezoelectric acoustic delay line and semiconducting sensor layer configuration. This will be the starting point to construct a multilayer analytical model, because a sensor layer with absorbed gas molecules may be treated as the sum of partial layers with a different electrical conductivity. Inside the sensor layer Knudsen's model of gas diffusion was used [26-28]. The analysis summarizes the acoustoelectric theory, i.e. Ingebrigtsen's formula [23,29], the impedance transformation law and gas concentration profiles, and predicts the influence of a thin semiconductor sensor layer with Knudsen's gas diffusion model on the SAW wave velocity in a piezoelectric acoustic waveguide in steady-state and non-steady-state conditions [30]. Basing on these results the sensor structure can be optimized. Some numerical and experimental results will be shown in the part 2 of this chapter.

2. Surface acoustic wave for semiconductor surface investigations

The fast development of micro- and nanoelectronics is connected with the development of various sensor and measurement techniques for semiconductor characterizations, and requires searching of new research methods. It seems that, the acoustic methods provide prospective possibilities of their applications in the technology of micro- and nanoelectronic devices. The surface acoustic wave methods may prove to be a useful, non-destructive tool for researches of the semiconductor surface in high and very high frequency ranges. Generally, these SAW methods are based on the interaction between the surface acoustic waves of the Rayleigh type and the free carriers in a semiconductor. This interaction is realised in the layered structure: the piezoelectric waveguide and the semiconductor [31-35] (**Figure** 1).

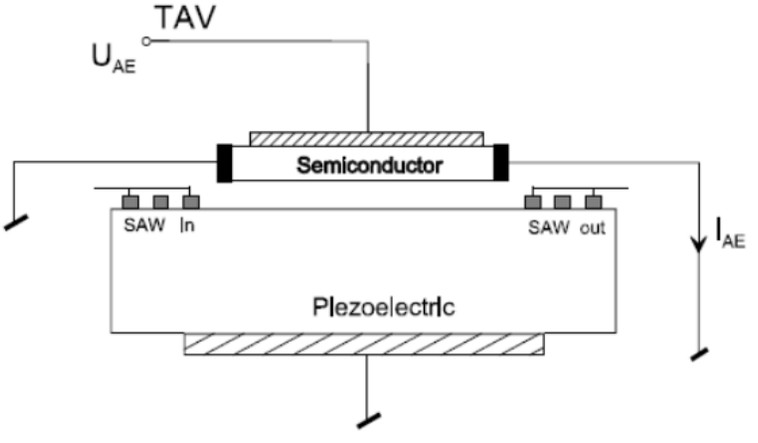

Figure 1. Piezoelectric-semiconductor structure for investigation of acoustoelectric interactions [35]

The electrical and electronic semiconductor surface properties may be determined by means of such parameters as: the surface potential, the carrier trapping velocity by fast and slow energetic surface states, the type of impurities of atoms and molecules, their concentration and location in the energy bandgap in the target material, as well as by the surface mobility of carriers and the lifetime of majority and minority carriers, the velocity of carriers trapping into surface states in semiconductor, and the effective live time of electrical carriers in fast surface states [36-39].

In the technology of electronic devices, silicon is a commonly applied material, but the III-V group semiconductors become more and more popular and important. This follows from the very interesting optical properties of these new materials. The coherent and non-coherent light sources were elaborated by using the electroluminescence effect observed in GaAs, GaP, InAs, InSb. Nowadays, special interest is devoted to the InAs semiconductor. The special electrical and electronic InAs properties arise mainly from the very high mobility of carriers, makeing it possible to construct electronic devices in very high frequency ranges. Applying the galvanomagnetic effect in InAs the hallotrons and gaussotrons were constructed [36]. This material is also often used in various sensors applications [6, 40].

Among the methods of semiconductor surface investigations, there are no methods which determine the surface parameters in high frequency ranges. The existing high frequency field effect method is used to deremine the kinetic parameters of near-surface regions, but its possibility of measurements is practically restricted to some MHz [1,5,41].

For this reason surface investigations of silicon and composed semiconductors in the high frequency range have not been performed. This gap can fill the methods based on SAWs.

2.1. Changes of SAW propagation conditions in results of acoustoelectric interaction

When the surface acoustic wave (SAW) propagates in a layered structore: piezoelectric – semiconductor, the electric field which accompanies this wave, penetrates the near- surface region of the semiconductor (**Figure** 1). The penetration depth of the electric field inside the semiconductor is of the order of the semiconductor extrinsic Debye length or the acoustic wavelength (whichever is shorter) [33, 42]. This electric field changes the free carrier concentration in the near-surface region of the semiconductor and causes a drift of the carriers [34,43]. Interaction of a surface acoustic wave (propagating on the border: piezoelectric crystal - semicondictor) with electrical carriers in the semiconductor may cause two types of effects. The first type forms effects observed in piezoelectric – changes of the velocity of SAW and changes of its attenuation [44]. The second type of effects are so called the acoustoelectric effects, observed in semiconductors [45,46].

Below the acoustic method of determining some parameters of fast surface states in semiconductors will be presented. This method is based on so-called interactions of the phonon-electron type [47] for determining both the effective carrier life-time τ influenced by the fast surface energetic states and the velocity g of the carrier trapped by the surface states.

As mentioned above, among the methods of investigations of semiconductor surfaces, there are no methods of investigating the kinetic properties of electrical carriers in fast and very fast surface states [1]. The existing methods allow only to investigate the surface sates with a carrier life-time τ of above 10^{-6}s [5,6]. In the case of extrinsic semiconductors the surface states may, however, be considerably faster (the carrier life-time in surface traps is usually less than 10^{-8}s). The existing electrical and spectroscopic methods of determining the parameters of fast surface states allow only to estimate these parameters, since the obtained results exhibit a considerable uncertainty. For this reason, investigations of the kinetic properties of fast surface states are not popular and there are not any new results concerning their determinations.

Problems connected with the determination of the chemical and mechanical procedures of surface treatments in the first step of preparation of semiconductor plates (wafers) for technology on their electron kinetic properties have rarely been taken up. The elaborated method is based on the phenomena of surface acoustic wave SAW propagation in the system: piezoelectric waveguide-semiconductor. The electric field, which accompanies a surface wave in the piezoelectric waveguide, penetrates the semiconductor to a depth equal to Debye's screening length [32,33]. Thus, the interactions of the acoustic wave and electrical carriers are manifested in the semiconductor in the form of acoustoelectric effects [34] and in the piezoelectric waveguide - by an additional SAW attenuation (the so called - electron attenuation) and by changing the velocity of the acoustic wave [38] **Figure** 2.

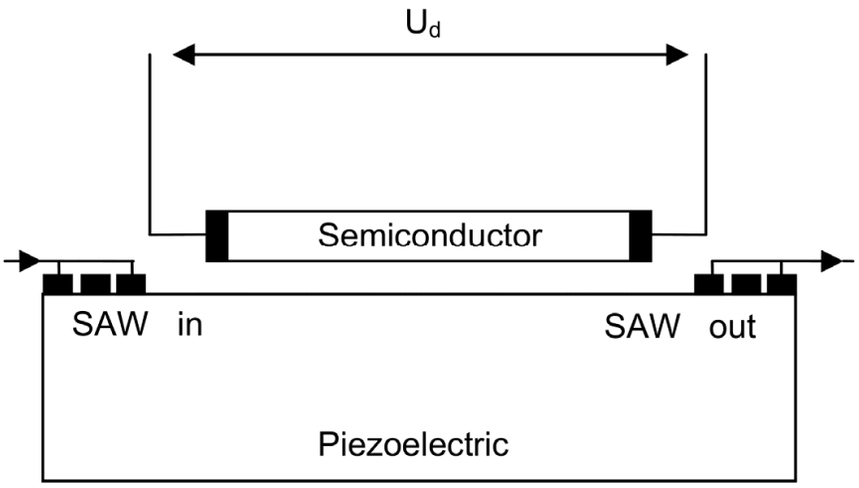

Figure 2. The idea of the piezoelectric waveguide-semiconductor system for investigations of the near-surface region in semiconductors [33]

Let us consider the surface wave which propagates on a piezoelectric waveguide in the system presented in **Figure** 2. The external electric drift field is applied to the semiconductor in the same direction. The coefficient of the electron attenuation of the surface wave α_e in such a system may be presented by the formula [33]:

$$\alpha_e = \frac{\eta \cdot \frac{\varepsilon_1}{\varepsilon_2} \cdot \frac{\omega}{\omega_c}(\gamma + a)\left[1 + \frac{\gamma + a}{A_D \cdot \frac{\omega}{\omega_c}\left[(\gamma + a)^2 + b^2\right]}\right]}{\left[1 + \frac{\omega}{\omega_c}\left(1 + \frac{\varepsilon_1}{\varepsilon_2}\right)b\right]^2 + \left[(\gamma + a)\left(1 + \frac{\varepsilon_1}{\varepsilon_2}\right)\frac{\omega}{\omega_c}b\right]^2} H \tag{1}$$

where:

$$a = \frac{g}{v_w} \cdot \frac{(\omega \cdot \tau)}{1 + (\omega \cdot \tau)^2} \tag{2}$$

$$\gamma = 1 - \frac{\mu_o \cdot E_d}{v_w} \tag{3}$$

$$A_D = \frac{1 + L_D^2 \cdot k^2}{L_D^2 \cdot k^2} \tag{4}$$

$$b = (\omega \cdot \tau) \cdot a \tag{5}$$

and v_w is the velocity of SAW, E_d the electric drift field, μ_o the mobility of electrons inside semiconductor, L_D the Debye length, k the wave number of SAW, ω the angular surface wave frequency, ω_c the so called "frequency of Maxwell's conductivity relaxation," η the square of the electromechanical coupling coefficient, γ the drift parameter, ε_1, ε_2 the permittivity of waveguide and semiconductor, respectively, g the velocity of carriers trapping into surface states in semiconductor, τ – the effective live time of electrical carriers in fast surface states, H – constant, the value of which depends on the elastic and piezoelectric properties of the waveguide and investigated semiconductor.

The process of electrical carriers trapped in the surface states in a semiconductor, under the influence of a surface wave which propagates in a piezoelectric crystal, was considered in detail in the paper [47]. **Figure** 3 presents changes of electron attenuation in the external electric field E_d in the semiconductor.

The critical electrical drift field is a field at which the electron attenuation of the wave is equal to zero:

$$\alpha_{cr}(E_{dkr}) = 0 \tag{6}$$

In [47] it was shown that the equation for the critical drift field takes the following form:

$$E_{d_{kr}} = \frac{v_w}{\mu_0}\left[1 + \frac{\omega \cdot \tau}{1 + (\omega \cdot \tau)^2}\right] \tag{7}$$

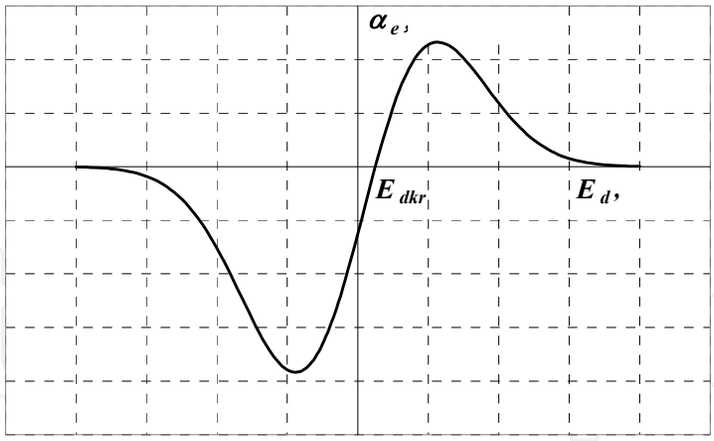

Figure 3. Electron attenuation α_e of a surface acoustic wave in the function of an external electric field E_d [47]

Accordingly

$$E^o_{d_{kr}} = \frac{v_w}{\mu_o} \tag{8}$$

where $E^0_{d_{kr}}$ is the critical drift field for the theoretical case, when no surface states exist in the semiconductor surface. From equations (7) and (8) it follows that the relative change of the critical drift field in real structure, caused by surface states, is given by:

$$\frac{E_{d_{kr}} - E^o_{d_{kr}}}{E^o_{d_{kr}}} = \frac{\Delta E_{d_{kr}}}{E^o_{d_{kr}}} = \frac{g}{v_w} \cdot \frac{\omega \cdot \tau}{1 + (\omega \cdot \tau)^2} \tag{9}$$

This relation is presented in **Figure** 4.

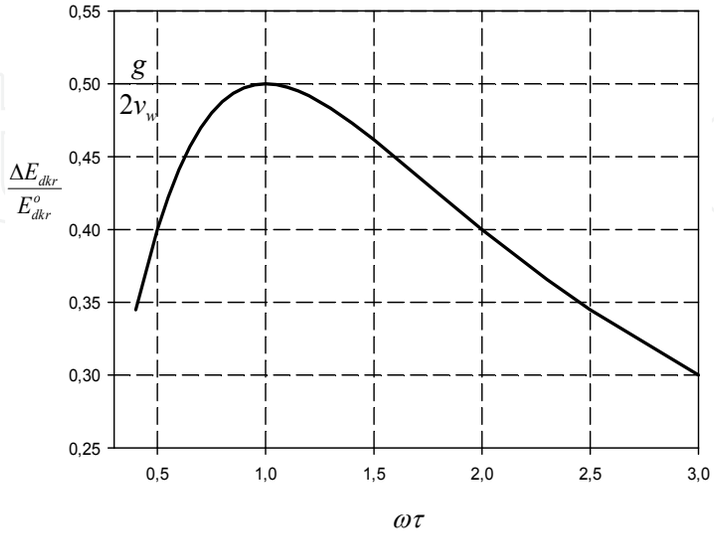

Figure 4. The characteristics $\frac{\Delta E_{dkr}}{E^o_{dkr}} = f(\omega\tau)$ [47]

The idea of assigning the parameters τ and g of surface states consists in the determination of the electron attenuation coefficient as the drift field function for different frequencies of the surface waves. From the characteristics $\alpha_e = f(E_d)$ can be determined E_{dkr} for each angular frequency ω; the next one determines the characteristics $\Delta E_{dkr} / E^o_{dkr} = f(\omega)$ and the last one calculates the carrier life-time τ in the surface states as (**Figure** 4):

$$\tau = \frac{1}{\omega} \tag{10}$$

The velocity of trapping of the carriers g in fast surface states is defined by the relation (Fig. 3):

$$g = 2v_w \left[\frac{\Delta E_{dkr}}{E^o_{dkr}} \right]_{\max} \tag{11}$$

If, therefore the surface wave propagates in the structure of a piezoelectric waveguide-semiconductor, two essential parameters of surface states in a semiconductor can be determined by measurements of the velocity and attenuation of the SAW.

2.1.1. Experimental set-up

As piezoelectric waveguides the lithium niobate $LiNbO_3$ plates (propagation plane [Y] with the wave propagation direction [Z]) were used. The idea of the experimental set-up is presented in **Figure** 5. The waveguide system permitted to perform the investigations at the frequency range: 2 – 350 MHz, by using some $LiNbO_3$ plates with the SAW transducers, obtained photolithographically. The application of a monochromator in the set-up permits to illuminate the semiconductor surface and to realise investigations of semiconductor plates for various semiconductor photoconductivities.

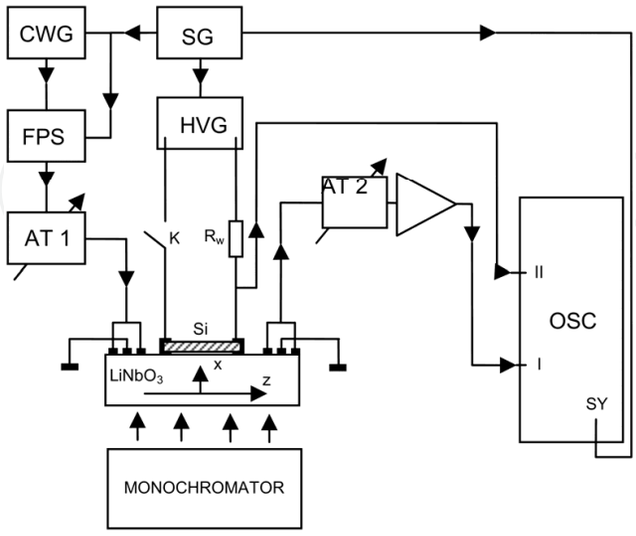

Figure 5. The scheme of the system for monitoring the electron attenuation coefficient αe as a function of the drift field Ed; (SG – synchronous generator, CWG – continuous wave generator, FPS – forming packet system, AT –attenuator, OSC – digital oscilloscope) [47]

The presented results concerning the plates of Si with the following parameters were obtained:

- Si[111], n-type, electrical conductivity $\sigma = 1{,}2[\Omega m]^{-1}$, volumetric mobility of the carrier $\mu_o = 0{,}13[m^2/V{\cdot}s]$, and the geometrical dimensions $10\times7\times0{,}05mm^3$.

The characteristics of $\alpha_e = f(E_d)$ for the real Si(111) surfaces after changing their electrical conductivity by means of optical excitations are presented in **Figure** 6. The measurements were performed for the following photoconductivities of the Si sample: $\sigma_1 = 1{,}2\ [\Omega m]^{-1}$; $\sigma_2 = 1{,}6\ [\Omega m]^{-1}$; $\sigma_3 = 1{,}9[\Omega m]^{-1}$.

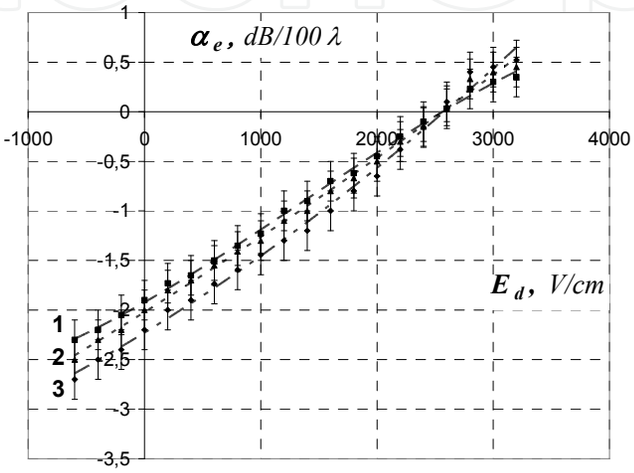

Figure 6. The experimental characteristics $\alpha_e = f(E_d)$ for the real surfaces of Si(111) concerning various photoconductivities: (1) $\sigma_1 = 1{,}2\ [\Omega m]^{-1}$; (2) $\sigma_2 = 1{,}6\ [\Omega m]^{-1}$; (3) $\sigma_3 = 1{,}9\ [\Omega m]^{-1}$ [47]

2.1.2. Results of investigations of fast surface state parameters in the Si single-crystal samples

By means of the method presented above the parameters τ and g for the Si single-crystal samples were determined whose surfaces were treated in various way.

Figure 7 presents the characteristics $\Delta E_{dkr} / E^{o}_{dkr} = f(\omega\tau)$ of the Si samples, but after their heating in vacuum at elevated temperature (~600K) as well as after heating at elevated temperature (~600K) but in atmosphere with saturated vapour. On the base of these investigations one can see that the parameters τ and g in Si are essentially different.

The results of these investigations are presented in Table 1.

The approximate values of the fast surface states concentrations N_t are quoted in Table 1. The procedure of N_t determination is based on the well known relation [1]:

$$g = S_n \cdot V_T \cdot N_t \tag{12}$$

where: V_T is the thermal velocity of electrons in semiconductors and S_n is the effective cross-section for electron trapping.

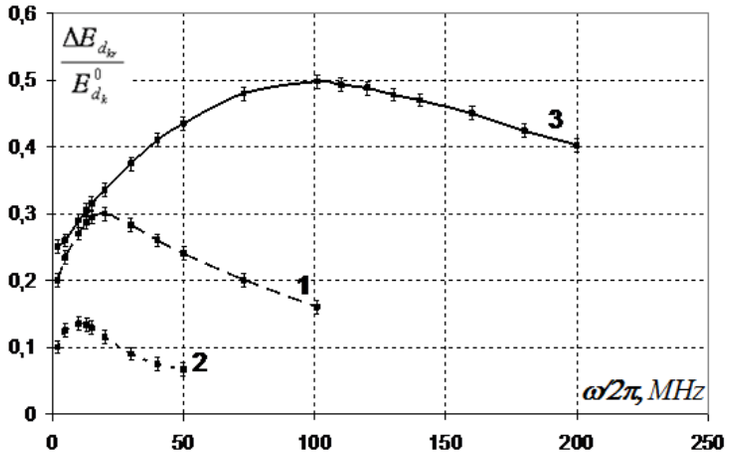

Figure 7. Relative changes of the critical field $\Delta E_{dkr} / E^{o}_{dkr} = f(\omega\tau)$ in Si(111): (1) in vacuum; (2) after heating in vacuum at ~600K; and (3) heating in steam at ~600K [47]

In the case of the Si single-crystals at room temperature the parameter S_n is approximately equal to ~$3 \cdot 10^{-16}$cm^2 [1,6]. Therefore the surface concentration N_t of the fast surface states can be estimated in tested semiconductors. The concentrations N_t are of the order 10^{13}cm^{-2} and depend considerably on the type of surface treatments.

Parameters of Si(111)	in vacuum	after heating in vacuum	after heating in water vapour
τ, s	$8{,}0 \cdot 10^{-9}$	$1{,}6 \cdot 10^{-8}$	$1{,}8 \cdot 10^{-9}$
g, m/s	1000	450	3400
N_t, cm^{-2}	~$3 \cdot 10^{13}$	~$1 \cdot 10^{13}$	~$8 \cdot 10^{13}$

Table 1. Parameters of the fast surface states in Si(111) [33]

2.1.3. Conclusion

The results presented above concerning the interaction between the surface acoustic wave in piezoelectric crystal and the electrical carriers in semiconductor have shown that the acoustic method can be applied to determine the parameters τ and g in investigations of the fast surface states in semiconductors.

The analysis of the method shows that the accuracy of the obtained results is better 5%, which is a rather good accuracy in the determination of the parameters of fast surface states. It can be pointed out that this method permits dynamic measurements of the surface state parameters over the frequency range up to several hundreds MHz (or even to some GHz), also for different, programmable changed photoconductivity of the tested semiconductors.

2.2. Acoustlectric effects in applications for semiconductor surface investigations

In a semiconductor, as a result of interaction between the electric carrier and the surface acoustic waves (SAW) the followning phenomena may be observed (**Figure** 1):

a. an electric current in the direction of surface wave propagation (i.e. longitudinal acoustoelectric effect LAE) [34],
b. a difference of electric potential between the semiconductor surface and its bulk (i.e. transverse acoustoelectric voltage TAV) [43].

In [26] the theoretical analysis of both acoustoelectric effects (LAE and TAV) was presented. These results formed the theoretical basis for new acoustic methods of determining the surface potential in semiconductors [46].

The experimental results of the surface potential as well as the lifetime of minority carrier investigations in some GaAs and GaP crystals performed by means of longitudinal and transverse acoustoelectric methods have been presented in [44,45].

The transverse acoustoelectric effect seems to be particularly important in semiconductor investigations. From its theoretical analysis [34, 44] it results that in the semiconductors in which one type of conductivity is predominant (n- or p-type), the sign of the acoustoelectric voltage depends on the type of electrical conductivity in the near-surface region. If the surface conductivity is negative (n-type), the transverse acoustoelectric voltage (TAV) has a positive value and if the surface conductivity is of the p-type, the value of TAV is negative. The results of investigations of the conductivity type in GaP and InP crystals have been presented in [46]. The measurement of the sign of TAV voltage is a fast and very easy method of determining the surface conductivity type.

The transverse acoustoelectric method of semiconductor surface investigations (based on the transverse acoustoelectric effect) is nondestructive. It does not require ohmic contacts on the investigated samples but, first of all, the method provides values of the surface parameters obtained at high frequencies.

Some samples of semiconductors of the III-V group were investigated by means of the TAV method. In [35] the investigations of semi-insulating GaAs at a low temperature and with a different surface wave power were reported.

Using the TAV methods we studied different semiconductor crystals, such as: GaAs [32], GaP [48], InP [45] crystals. To our knowledge, there are no papers dealing with these methods of surface investigations.

Further on, in this chapter the experimental results of the surface investigations of InAs (111) crystals after various surface treatments are quoted, as well as the results of the theoretical analysis of TAV concerning the surface electrical conductivity and surface potential.

2.2.1. Experimental

The set-up for investigations of the surface semiconductor by means of the transverse acoustoelectric method is shown in **Figures** 8 and 9. The layered structure consists of the tested semiconductor is presented in **Figures** 8a and 8b [42,48].

The short (some μ-seconds) impulses of 134 MHz are applied to the input interdigital transducer to generate surface acoustic waves (SAWs) on the Y-cut, Z- propagating in LiNbO3 delay line. The semiconductor is placed on the surface of the delay line in an isolating distance bars in order to assure a non-acoustic contact between the semiconductor and the piezoelectric waveguide. The transverse acoustoelectric signal (TAV) across the semiconductor is detected by placing one Al plate on the back surface of the semiconductor (TAV electrode 2), and another one under the semiconductor sample placed on the acoustic wave guide (TAV electrode 1). The thickneses of the TAV electrode 1 and the isolating distance bars amounts to about 400 nm.

In order to provide the best contact between the investigated semiconductor surface and the TAV electrode 1, this electrode consists of narrow strips (**Figure** 8b). The width of a single metallic strip is ~ $2 \cdot 10^{-2}$ mm and the distances between them are about 0.5 mm.

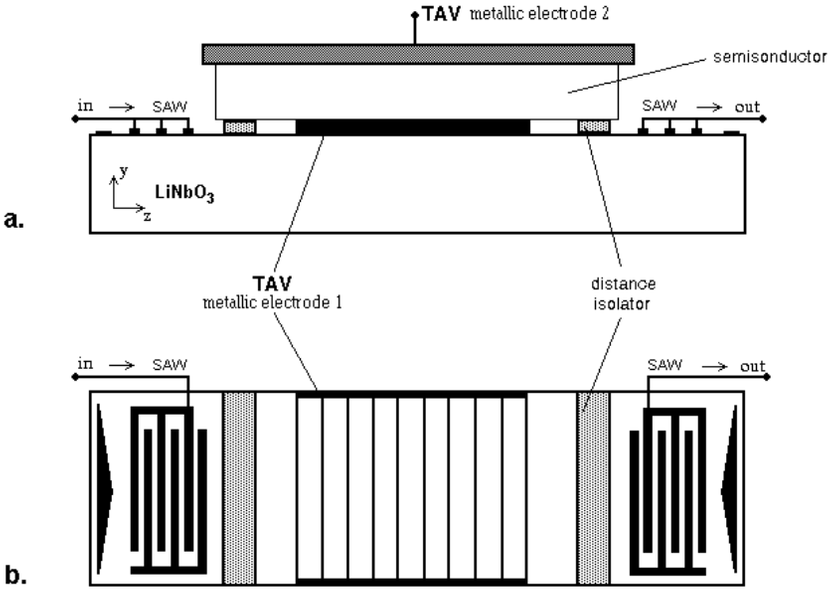

Figure 8. a,b. Schematic presentation of the layered structure: piezoelectric wave guide and investigated semiconductor [42]

The distance between the strips is much larger than the acoustic waveength ($\lambda \approx 2.5 \cdot 10^{-2}$ mm), and for this reason the TAV electrode 1 is not essential for the SAW propagation and does not disturb it. The TAV electrode 1 in the form of a grating provides a good electric field distribution between both TAV electrodes. It relates to acoustoelectric voltage as well as to external voltage U_d.

In order to change the value of the surface potential in the investigated semiconductor, we applied to the semiconducter a d.c. voltage or the pulse voltage across the TAV electrodes. The set-up is shown in **Figure** 9.

For registration of the acoustoelectric voltage, in our set-up we used the digital scope (IWATSU DS-86359) and the computer scope converter(PFS-20).

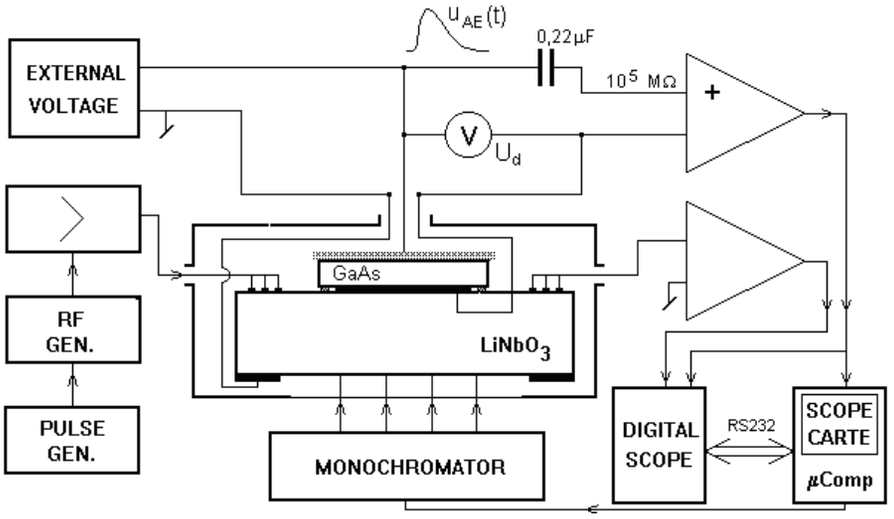

Figure 9. The experimental set-up for investigations of the semiconductor surface by means of theTAV method [42]

Using the higher harmonics of the acoustic transducer it is possible to investigate semiconductors above one GHz.

The interdigital transducers and the aluminium TAV electrode 1 are produced by standard evaporation and photolithography techniques.

The transverse acoustoelectric voltage method was used to investigate the InAs (111) crystal samples with the following bulk parameters:

- n-type electrical conductivity;
- carrier mobilities: $\mu_n = 33\,000$ cm^{2}V^{-1}s^{-1}; $\mu_p = 460$ cm^{2}V^{-1}s^{-1}permittivity: $\varepsilon = 11.5$;
- band gap : Eg = 0.44 eV,
- electron concentration: $N_d = 1.6 \circledcirc 10^{15}$ cm^{-3},
- resistivity: $\rho = 2.5 \circledcirc 10^5$ Ωcm.

2.2.2. Results and discussion

In [49] we presented the results of our theoretical analysis of the acoustoelectric effects (longitudinal acoustoelectric current and transverse acoustoelectric voltage) in a layered piezoelectric - semiconductor structure. We have shown the theoretical relations between the acoustoelectric voltage and the semiconductor surface parameters such as the surface electrical conductivity and the surface potential. **Figure** 10 presents the transverse acoustoelectric voltage (TAV) as a function of surface electrical conductivity in the investigated InAs sample.

This function was calculated by means of our theoretical results presented in [49]. At some values of the p-type surface conductivity the minimum transverse acoustoelectric voltage is observed (about $\sigma \approx 10^{-4}$ 1/Ωcm). In the case of the p-type surface electrical conductivity the TAV amplitudes have negative values. Then, starting from $\sigma \approx 10^{-2}$ 1/Ωcm, the amplitude

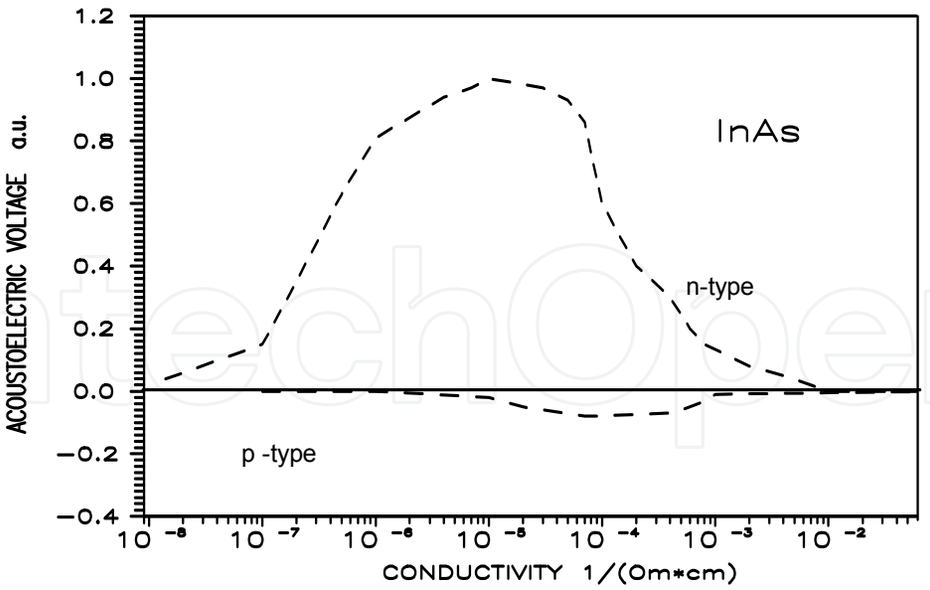

Figure 10. Transverse acoustoelectric voltage as a function of the electrical surface conductivity in InAs [49]

TAV is equal to zero up to $\sigma \approx 10^{-8}$ 1/Ωcm n-type surface conductivity. Next, the TAV starts to grow, it has positive values of TAV amplitude and reaches the maximum at $\sigma \approx 10^{-5}$ 1/Ωcm. For higher values of conductivity the TAV grows small and for $\sigma \approx 10^{-2}$ 1/Ωcm it is practically equal to zero. The qualitative explanation of the dependence of this kind is simple. For very high carrier concentrations, near the intrinsic region, the interactions between the electric field (accompanied the acoustic wave in piezoelectric waveguide) and carriers in the near-surface region are very weak. The TAV, as the results of these interactions are also very small. In the opposite case, if the carrier concentration in the semiconductor is high, the electric field of the wave is practically complet screened by these carriers. Then, the TAV amplitude is also small. One can see in **Figure** 10. that the transverse acoustoelectric voltage spectroscopy is a very sensitive method for high resistivity semiconductors. It is an ideal technique to study the InAs samples, because their electrical properties (high resistivity and high carrier mobility) are just in the high sensitivity TAV range.

As it was mentioned before, the electronic properties of the near-surface region may be changed by external electrical voltage perpendicular to the surface. It is a very simple method of influencing the surface semiconductor properties. In **Figure** 11 the experimental dependence of the amplitude of the transverse acoustoelectric voltage U_{AE} upon the external voltage U_d for InAs sample is presented.

Figure 12 shows the theoretical function of the amplitude of TAV versus the surface potential U_S for InAs singlecrystals.

U_S denotes the value of the surface potential in kT units: $U_S = e\Phi_S/kT$ and Φ_S denotes the surface potential in the semiconductor [6] (in Volt unites).

The function presented in **Figure** 12 was calculated basing on the theoretical relations quoted in [49]. In order to determine this relation, we had to know the following bulk parameters presented above: the mobility concentration of the carriers, the permittivity and the electrical conductivity for the investigated InAs crystals.

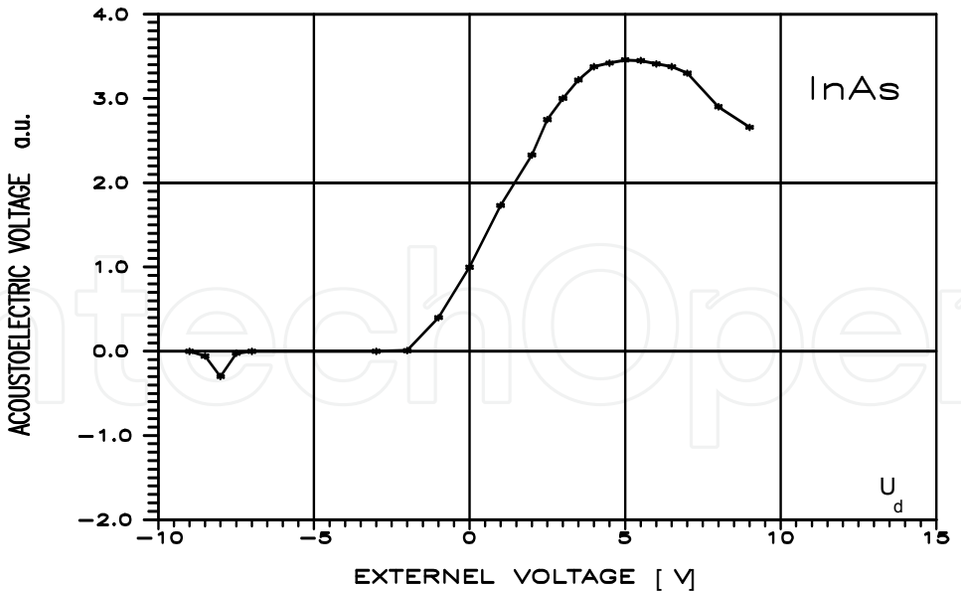

Figure 11. The experimental dependence of U_{AE} on the external voltage U_d for InAs surface

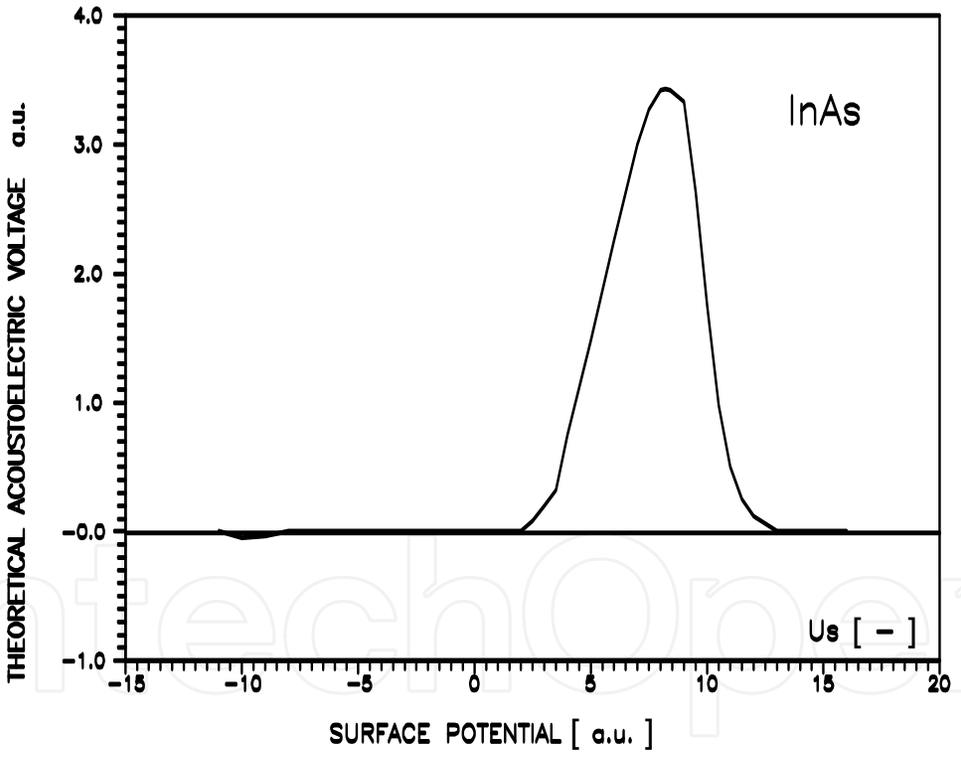

Figure 12. The theoretical dependence of U_{AE} on the surface potential U_S for InAs ($U_S=e\Phi_S/kT$) [49]

By using both functions: the experimental relation $U_{AE} = f(U_d)$ and the theoretical relation $U_{AE} = f(U_S)$, one may propose the method of determining the surface potential value in semiconductors (for zero external bias voltage). This method of determining the surface potential was discussed in detail in [45].

The theoretical dependence of the TAV amplitude upon the surface potential U_S is calculated with an accuracy up to an arbitrary constant multiplier K [45]. (The constant K

may be interpreted as a so called aperture constant). For K we may substitute the value for which the maximum in the theoretical relation $U_{AE} = f(U_S)$ and the maximum in the experimental relation have the same values. For the experimental characteristic $U_{AE} = f(U_d)$, the value $U_{AE} = 1$ corresponds to the case for which the external voltage U_d is equal to zero. For the theoretical relation $U_{AE} = f(U_S)$, the value $U_{AE} = 1$ corresponds to the surface potential of the investigated semiconductor sample.

For the investigated InAs sample, the value of the surface potential Φ_S obtained by applying this method was equal to $\Phi_S = - 0.11 \pm 0.02$ V [49].

The transverse component of the electric field of the acoustic wave in the piezoelectric waveguide acting on electrical carriers in semiconductors changes its concentration in the near-surface region. The new steady state of the concentration is reached after the time period which depends on the carrier lifetime. The properties of the electrical surface semiconductor differ from the bulk ones. Therefore, the values of lifetime in the bulk and in the surface may be quite different, too.

The lifetime of the minority carriers may be determined from the shape of the transverse acoustoelectric signal. It was shown in [49] that the transverse acoustoelectric signal $u_{AE}(t)$ is described by the following mathematical formula:

$$u_{AE}(t) = U_{AE} \frac{t}{\tau_a - \tau_e} \left[e^{-t/\tau_a} - e^{-t/\tau_e} \right] \tag{13}$$

where:

U_{AE} - transverse acoustoelectric amplitude,

τ_a - time constant of the experimental set-up,

τ_e - effective life time of the minority carriers.

For the case, when the time constant of the experimental set up τ_a is much longer than the life time of minority carriers ($\tau_a >> \tau_e$), the value of the time constant of the acoustoelectric signal is practically equal to the life time of minority carriers τ_e.

(The condition $\tau_a >> \tau_e$ is usually easy to be satisfied). The life time τ_e was determined making use of this method. For the InAs sample under investigation the life time of the minority carriers is equal to $\tau_e = 2.0 \cdot 10^{-4}$ s (before the surface treatment).

The experimental measurements of the TAV amplitude versus the surface acoustic wave power allow to estimate the intensiy of the influence of the surface processes on the total conductivity of the investigated samples. If the interactions between the electric carriers and surface traps are not intensive, the amplitude U_{AE} versus the acoustic power of the surface acoustic wave is a linear function. If the interactions of the electric carriers with the surface tarps are intensive, relation $U_{AE} = f(P_{ak})$ is non-linear [42].

The very important advantage of the method based on the transverse acoustolectric effect is the possibility of checking the semionductor surface in the course of the alteration of the surface properties. We think that this fact will allow to control the changes of the surface parameters after various surface treatments due to the technological process.

In [44,45] we presented the results of the determination of the surface potential, the life time of the minority carriers, and the type of electrical conductivity obtained for Si, GaP and GaAs single-crystal samples, which vary in their bulk and surface properties.

The main purpose of these investigations was to explore the influence of the surface treatments for the values of the surface parameters. The samples were measured after mechanical and chemical surface treatments which are applied during the technology of electronic devices. We also tested the surface parameters after mechanical grinding with alumna powders of various granulations and after polishing with diamond paste. We also tested the surface parameters after the cleaning of the sample in acetone, benzene, methanol and after chemical etching in HF acid or in $3HNO_3 + 10H_2O_2$. After the surface treatments, the samples were rinsed in methanol and deionized water. We applied various combinations of simultaneous mechanical and chemical treatments.

Figure 13 presents the changes of life time of the minority carriers in the InAs sample after: a) grinding with alumna powder (grains No100) , b) diamond paste polishing, c) HF acid etching [49].

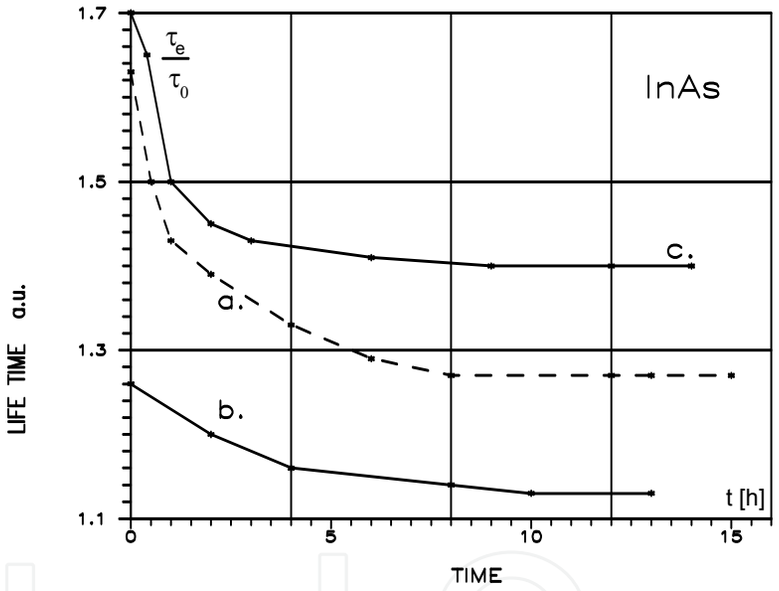

Figure 13. The life time of minority carriers in InAs after different surface treatment: a) alumna powder grinding, b) diamond paste polishing, c) HF acid etching [49]

In these studies we observed that the life time of the carriers changed very essentially after alumna powder grinding.

The changes of τ_e stopped after some hours, but with different steady state values than before the surface treatments.

The steady state value of the minority carriers life time after grinding with alumna powder is equal to $\tau_e = 2.5 \odot 10^{-4}$ s. In **Figure** 13, the time τ_0 denotes the steady state of life time of the minority carriers before the surface treatments, equal to $\tau_o = 2.0 \odot 10^{-4}$ s.

The very long time of the transient state of the life time shows that in the surface processes not only fast surface states take part but also slowl surface states in the oxide layer.

2.2.3. Conclusion

It follows from the presented results that the transverse acoustoelectric method (TAV) is useful tool for studying the electrical and electron surface properties of semiconductors. On the example of IaAs (111) it was shown, that the TAV method allows to determine experimentally the surface potential and the effective live time of minority carriers, as well as the type of the surface conductivity in the near-surface segion. Indium arsenide is a relatively new semiconductor material. This material is used, among others, in the technology of luminescence and electroluminescense devices, as well as target material for laser diodes, hallotrons and gaussotrons.

Basing on the theory of acoustoelectric effects, one can present also the results of the theoretical analysis ofr TAV versus the surface potential. These theoretical results and the experimental relation U_{AE} versus the external voltage U_d allowed to determine the value of the surface potential in the investigated InAs sample by zero bias voltage.

In the case of the IaAs (111) sample the surface potential determined by means of our acoustic method was equal to $U_S = - 0.11 \pm 0.01$ V.

We presented the theoretical results of the acoustoelectric voltage versus the electrical conductivity in the near-surface region. It follows from this result that TAV is a very strong function of the carriers concentration and only in the case of restricted concentration partitions the TAV amplitude differs from zero value. In the investigated InAs (111) sample these concentrations are in the range: $1.3 \cdot 10^{15} \div 7.0 \cdot 10^{16}$ cm^{-3}.

We proved that the values of τ_e depends on technology the type of technology of the surface preparation. The largest changes of τ_e in the InAs sample were observed in the case of mechanic alumna grinding (No 100) and for HNO_3 acid etching. The changes of τ_e after these surface treatments were of some tens percents. After cleaning and boiling in different alcoholes, benzene and acetone the changes of life times were less, only about some percents. The smallest changes of τ_e were observed after benzene cleaning (2-3 %). After diamond paste polishing the changes of τ_e amounted to about ten percents.

The Transverse Acoustoelectric Voltage Method is non destructive. Moreover, this method does not require ohmic contacts with the tested semiconductor samples. This method provides the possibility of determining the values of the parameters in high and very high frequency ranges.

The results presented above were obtained for surface acoustic wave frequency of 134 MHz. The surface semiconductors may be investigated by means of the SAW techniques up to some GHz. Results of the semiconductors surface investigations of III-V group in a very high frequency range have been presented in [48,49].

From the presented measurements it follows, that acoustic methods may be very useful complement for existing electrical, photospectroscopy and photoemission methods of semiconductor surface investigations.

3. SAW application in gas sensors

The SAW sensor set-up is based on frequency changes in a surface acoustic wave dual delay line system, which is nowadays well known – **Figure** 14.

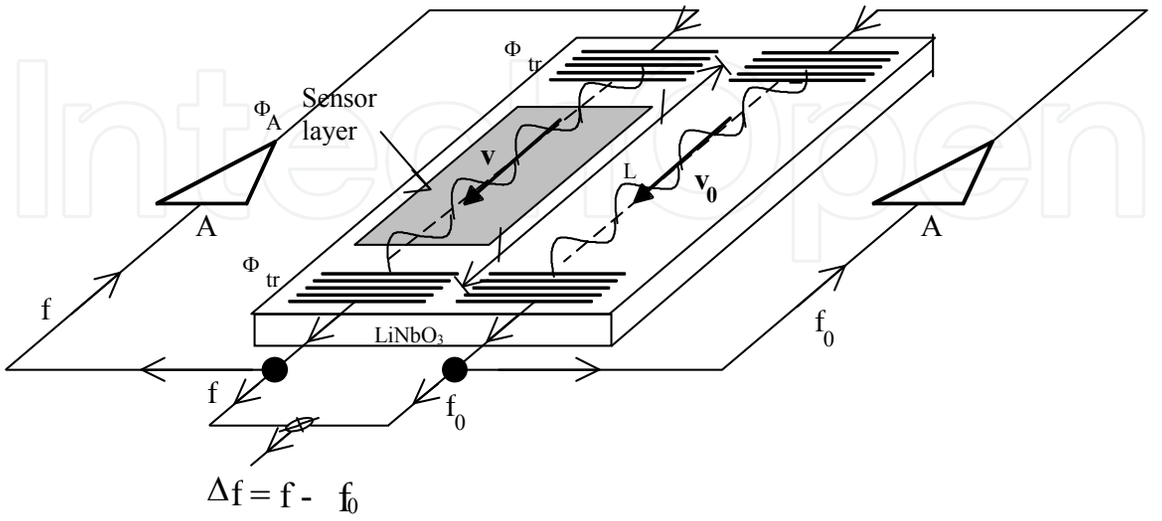

Figure 14. The SAW dual delay line system based on frequency changes. The abbreviations: Φ_A ,Φ_{tr} - phase shift introduced by amplifier and transducer respectively, A - amplifier; v, v_0 - velocity of the SAW in a measuring and reference paths [24]

On a piezoelectric substrate (usually $LiNbO_3$) two identical acoustic paths were formed using interdigital transducers [50]. Next an active multilayer sensor structure is formed in the measuring line by vacuum deposition processes. The second path serves as a reference and can compensate small variations of ambient temperature and pressure. Both delay lines are placed in the feedback loop of oscillator circuits and the response to the particular gas of the active multilayer is detected as a change in the differential frequency Δf, i.e. the difference between the two oscillator frequencies f and f_0.

Principally, any change in the physical properties of a thin active multilayer, due to its interaction with gas molecules on a piezoelectric surface can affect SAW propagation. However, from the practical point of view only the two following effects have a potential meaning. Namely, a change in the mass density of the multilayer, and a change in its electrical conductivity cause significant changes in the velocity and attenuation of the SAW and consequently changes in the frequency f and Δf .

At first, according to D'Amico [51], we used a palladium (Pd) layer as a sensitive material in experimental results. A palladium film absorbs easily hydrogen molecules and is a well known material for the detection of hydrogen. Hydrogen absorption and desorption cause changes in the density, elastic properties and conductivity of the Pd film. The process is completely reversible. The obtained result was unfortunately very weak – **Figure** 15. The changes of the frequency Δf do not exceed 50 Hz for 0.5 % and 1 % for hydrogen in nitrogen at 30 ^oC and this is almost the detection limit of the equipment. At higher temperatures there were no better results. When a 720 nm CuPc layer was used the sensor response amounted

to about 600 Hz, but only at higher temperatures than70 °C. The result is shown in **Figure** 16. It is also a well- known fact, that phthalocyanine films must be thermally activated to detect gas. The investigated CuPc layer with a thickness of about 720 nm was obtained by means of the vacuum sublimation method, using a special aluminium mask.

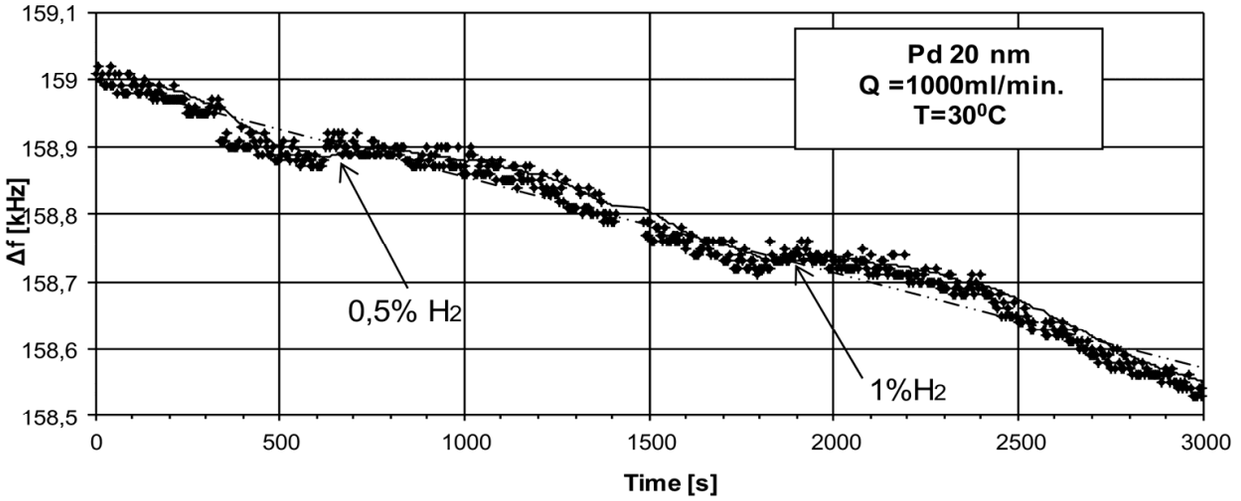

Figure 15. Changes of the differential frequency versus time at two concentrations of hydrogen for 20 nm of palladium at 30 ⁰C [51]

The source temperature was about 600 °C and the thickness was measured by the interference method. Before the specific process of sublimation, CuPc powder (Aldrich) was initially out-gassed at 200 °C for 15 to 20 min in vacuum (10^{-4} Torr). The CuPc vapour source was a crucible placed in a properly formed tungsten spiral. A copper-constantan thermocouple was used to control the temperature. In the case of multilayer structure the obtained results are very promising. We can observe recurrent changes of the differential frequency of the measurements system in the function of the medium hydrogen concentration in nitrogen at 30 °C and 50 °C of interaction – **Figure 16**.

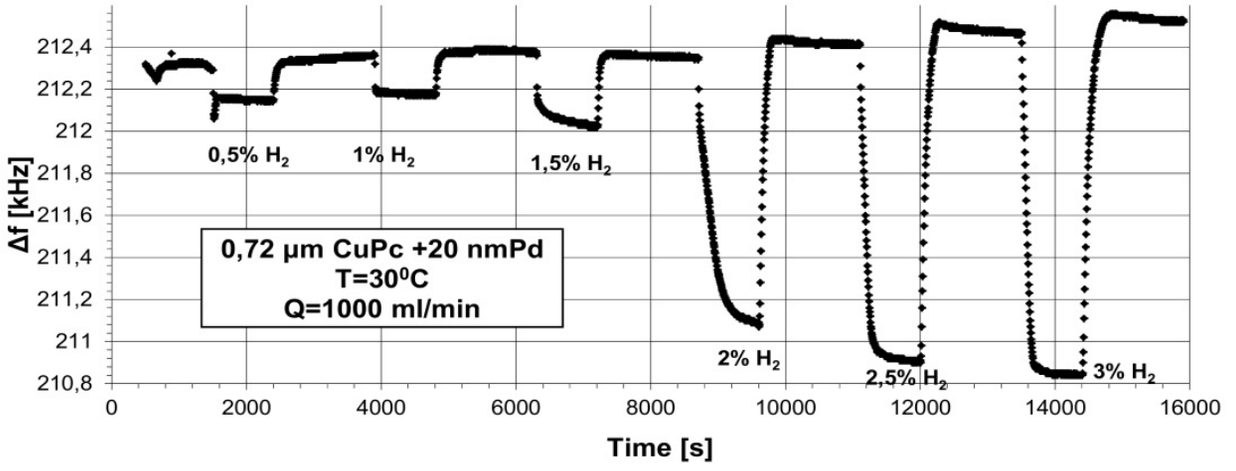

Figure 16. Changes of the differential frequency Δf versus time concerning a multilayered sensor structure at 30 ⁰C with different concentrations of hydrogen in nitrogen [24]

Such a good work of the sensor may be explained as follows. As already mentioned above, it is well known, that the palladium film easily absorbs hydrogen molecules. However, when we use only a metal (palladium) layer on a piezoelectric substrate (which was $LiNbO_3$ Y-Z), the metal layer shortens the electric field associated with the surface wave. Consequently, the sensor can detect only the mass loading. When only a CuPc layer is used, the sensitivity of this compound is too weak to detect hydrogen molecules, besides, the conductivity of the layer at room temperature is too high and this sensor must be temperature-activated. Nowadays it is well established, that in the case of phthalocyanine compounds in a SAW system the electric effect is much greater than the mass loading. So that, to take full advantage of the high sensitivity offered by the SAW sensor, the thin film conductivity must be in some particular range [25,52,53]. The multilayer structure (CuPc 720 nm + 20 nm Pd) on a $LiNbO_3$ Y-Z substrate has probably its resultant electrical conductivity well fitted to the high sensitivity range of the SAW device and can detect hydrogen molecules even at room temperature.

We have also used hydrogen phtalocyanine covered with a thin palladium film. Interaction results with hydrogen gas are shown in **Figure** 17.

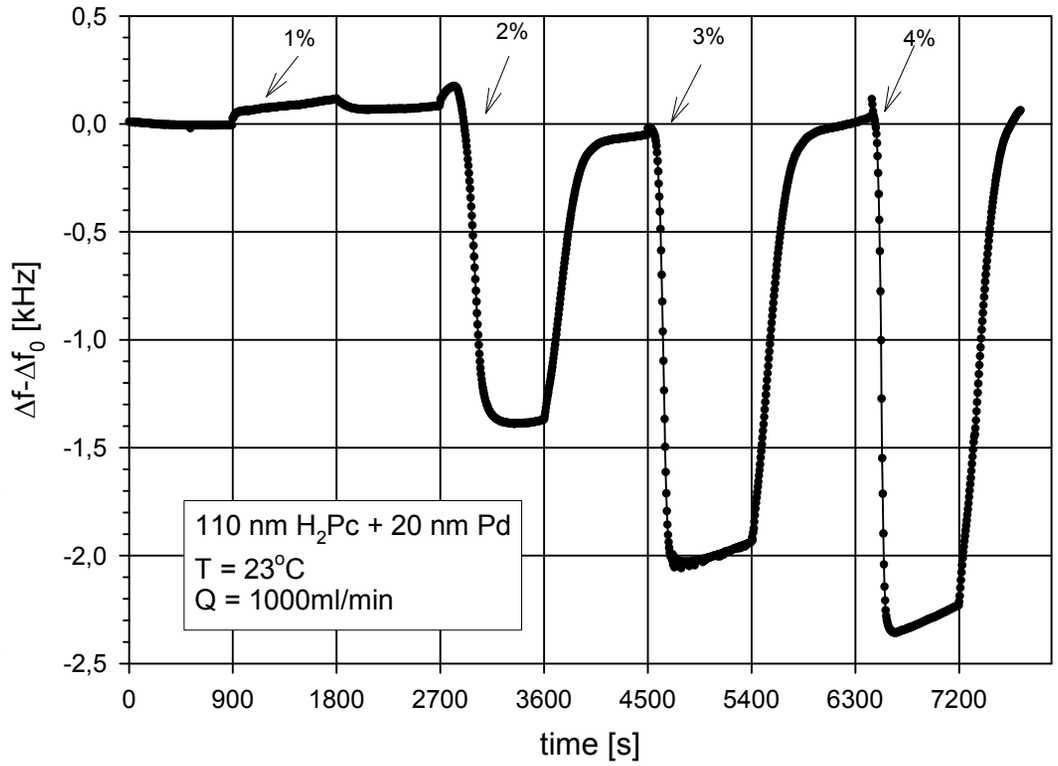

Figure 17. Changes of the differential frequency Δf versus time in a multilayered sensor structure at 23 ^{0}C and at different concentrations of hydrogen in nitrogen [52,53]

3.1. Acoustoelectric effect in the piezoelectric – semiconductor layer

In the case of small disturbances, both mass and the electric load mentioned above may be considered separately, assuming that the total effect of a relative change of the wave vector

$\Delta k/k_0$ and the velocity of propagation $\Delta v/v_0$, is the sum of both these component disturbances [22].

$$\frac{\Delta k}{k_0} \approx \left(\frac{\Delta k}{k_0}\right)_m + \left(\frac{\Delta k}{k_0}\right)_\sigma \tag{14}$$

Making use of the theory of disturbances [54], the contribution of each of these effects can be determinates theoretically. From the physical point of view it seems to be essential that the influence of each effect (mass and electrical) should be considered separately from its reaction to the interaction of the layer with gas. In the case of an electric effect we may assume that the mass of the layer is m=0. The electric "load" results from the effect of the interaction of the electric potential associated with the surface wave with mobile charge carriers in the layer.

3.2. Electrical surface perturbations

In these problems the mechanical boundary conditions are unperturbed. If the electrical boundary conditions are perturbed only at the upper surface y=0, the perturbation formula is [23,54]:

$$\left(\Delta k\right)_\sigma \approx \frac{\omega\left[\varphi'(0)D_y^*(0) - \varphi^*(0)D_y'(0)\right]}{4P} \tag{15}$$

where the index σ refers to the change of the wave number due to disturbances, electrical surface perturbations.

In these problems the mechanical boundary conditions (T=0) are unperturbed. Unperturbed electrical boundary conditions are usually neither a short-circuit [$\sigma(0)$ = 0] nor an open-circuit [$D_y(0)$=0]. The best agreement between the perturbation theory and exact numerical calculations is obtained by using the so-called weak coupling approximation, in which the stress field T is assumed to be unchanged by the perturbation.

We can define an impedance per unit area [30,55]:

$$Z_E(0) = \left(\frac{\varphi}{i\omega D_y}\right)_{y=0} \tag{16}$$

It will be assumed, that unperturbed problem provides free electrical boundary conditions at the substrate surface, that is, the region above the substrate (y<0 in **Figure** 18) is a vacuum and extends to y→ ∞. The space-charge potential satisfies the general form of Laplace. For this region Laplace's equation is reduced to [30]:

$$\nabla^2\Phi = 0 \tag{17}$$

The unperturbed potential function is therefore:

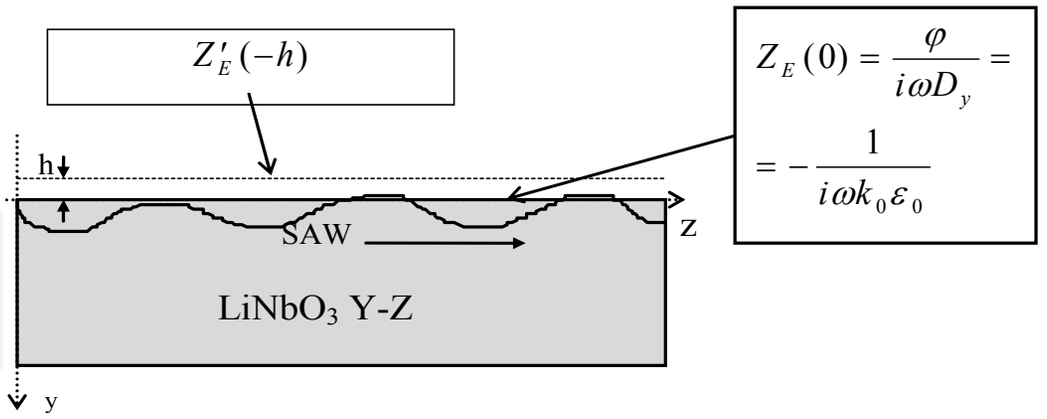

Figure 18. Electrical surface perturbations [30]

$$\Phi = \Phi_R(y)e^{-ikz} = e^{ky}e^{-ikz},\ y < 0 \tag{18}$$

and the normal component of electrical displacement is:

$$D_y = -k\varepsilon_0 e^{ky}e^{-ikz},\ y < 0 \tag{19}$$

Consequently, the unperturbed surface impedance is:

$$Z_E(0) = -\frac{1}{i\omega k_0 \varepsilon_0} \tag{20}$$

The perturbed boundary conditions will be specified in terms of the normalized surface impedance:

$$z'_E(0) = \frac{Z'_E(0)}{\left|Z_E(0)\right|} = -ik_0\varepsilon_0\left(\frac{\varphi'}{D'_y}\right)_{y=0} \tag{21}$$

The potential of the perturbed fields $\varphi'(0)$ and the electrical displacement $D_y(0)$ are now related to the unperturbed fields:

$$\begin{aligned} \varphi'(0) &= \varphi(0) + A \\ D'_y(0) &= D_y(0) + k_0\varepsilon_p^T A \end{aligned} \tag{22}$$

where

$$\varepsilon_p^T = \sqrt{\varepsilon_{yy}^T\varepsilon_{zz}^T - \left(\varepsilon_{yz}^T\right)^2}$$

and the approximation $k_0' = k_0$ has been made. The electrical displacements $D_y(0)$ and $D_y'(0)$ are expressed in terms of potential. At the end the electrical potential and induction may be expressed as:

$$\varphi'(0) = -iz'_E(0)\frac{\left(\varepsilon_0 + \varepsilon_p^T\right)}{\varepsilon_0 - i\varepsilon_p^T z'_E(0)}\varphi(0) \tag{23}$$

$$D'_y(0) = -\frac{k_0\varepsilon_0\left(\varepsilon_0 + \varepsilon_p^T\right)}{\varepsilon_0 - i\varepsilon_p^T z'_E(0)}\varphi(0) \tag{24}$$

At the end we obtain:

$$\frac{\Delta k}{k_0} = -\left(\frac{\Delta v}{v_0}\right)_{sc}\frac{1 + iz'_E(0)}{1 - i\dfrac{\varepsilon_p^T}{\varepsilon_0}z'_E(0)} \tag{25}$$

for the unperturbed boundary conditions (electrically free), and perturbation of the velocity due to an electrical short-circuit on the boundary (*sc*):

$$\left(\frac{\Delta v}{v_0}\right)_{sc} = -\omega\left(\varepsilon_0 + \varepsilon_p^T\right)\frac{\left|\varphi(0)\right|^2}{4P} \tag{26}$$

This is the Ingebrigtsen formula for electrical surface perturbations of SAW Rayleigh waves. It is also applicable to other types of piezoelectric surface waves when the appropriate normalized surface wave potential is used in $\left(\frac{\Delta v}{v_0}\right)_{sc}$. Since the unperturbed wave satisfies free electrical boundary conditions, then $\Delta k \to 0$ in (2.13) when:

$$z'_E(0) = \frac{Z'_E(0)}{\left|Z'_E(0)\right|} \to i \tag{27}$$

The influence of the effect between the electric potential associated with the acoustic wave and the carriers of the electric charge in this layer leads to a decrease of the velocity. This effect depends on the electromechanical coupling factor K^2. The Ingebrigtsen formula for electrical surface perturbations of SAW Rayleigh waves is reduced to the form [23,30]:

$$\left(\frac{\Delta k}{k_0}\right) = \frac{K^2}{2}\frac{1 + iz'_E(0)}{1 - i\dfrac{\varepsilon_p^T}{\varepsilon_0}z'_E(0)} \tag{28}$$

where

$$K^2 = 2\left(\frac{\Delta v}{v_0}\right)_{sc}$$

3.3. Infinitesimally thin semiconducting sensor layer

We consider first the RF interaction with an infinitesimally thin semiconductor, regarded to be thinner than the Debye length. For the width w in the x direction, the one-dimensional equation of motion is:

$$I_z = \rho_{01}\mu E_z - D\frac{d\rho_1}{dz} \tag{29}$$

where I_z is the total RF current in the direction z, ϱ_1 and ρ_{01} are, respectively, the RF and dc charge density per unit length. The quantities μ and D are, respectively, the carrier mobility and diffusion parameters. By combining the one-dimensional equation of continuity:

$$\frac{dI_z}{dz} + i\omega\rho_1 = 0 \tag{30}$$

with (2.17) and assuming that all RF quantities vary as exp[$i(\omega t - kz)$], it follows that the RF charge field is related by:

$$\rho_1\left(\omega - iDk^2\right) = k\rho_{01}\mu E_Z \tag{31}$$

Although thin, the semiconductor layer has a finite thickness h, width w and the volume dc charge density is:

$$\rho_0 = \rho_{01}\Big/wh$$

Following the conventions established by White [49] for the volume acoustic wave in configurations, where we define the relaxation frequency $\omega_c = \frac{\mu|\rho_0|}{\varepsilon}$ and the diffusion frequency $\omega_D = \frac{v_0^2}{D} = \frac{k_B T}{q}\mu$, where k_B - Boltzman's constant, T – temperature.

We then rewrite (31) in the form:

$$\rho_s = \frac{\left(\frac{\omega_c}{\omega}\right)\varepsilon kh}{1 - i\frac{\omega}{\omega_D}}E_z \tag{32}$$

where $\rho_s = \rho_1\Big/w$

3.4. Surface impedance of single semiconducting sensor layer

Figure 19 presents the schematic diagram of the layered SAW gas sensor.

When $y < 0$ in **Figure** 19, we assume isotropic conditions. The space-charge field boundary conditions for single semiconductor layer in the plane $y=0$ are respectively: $\varphi(0^-) = \varphi(0^+)$ and $D_y(0^-) - D_y(0^+) = \varrho_s$, where $D_y(0^-) = \varepsilon_0 E_y(0^-)$. Since we assume that the field solution has an electrostatic form $\vec{E} = -\nabla\varphi$, we imply that $E_z^- = ik_0\varphi(y,z)$.

By applying Gauss' law and potential continuity in the plane $y=0$, the impedance $z_E'(0)$ can be expressed in the following form:

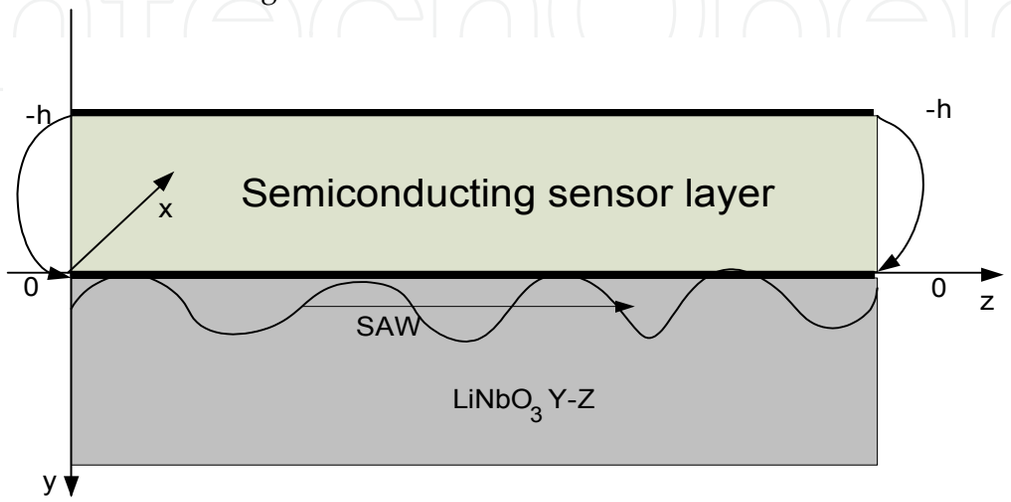

Figure 19. Schematic diagram of the layered SAW gas sensor [30]

$$z_E'(0) = \left(-i + \frac{\dfrac{\sigma_s}{\varepsilon_0 v_0}}{1 - \mathrm{i}\dfrac{\omega}{\omega_\mathrm{D}}} \right)^{-1} \tag{33}$$

where $\sigma_s = \sigma h$ is the surface conductivity of the layer.

In the case of the diffusion effects are small (D~0), the surface conductivity is independent of the frequency of the wave propagation and surface impedance $z_E'(0)$is only function of the surface conductivity σ_s

$$z_E'(0) = \left(-i + \frac{\sigma_s}{\varepsilon_0 v_0} \right)^{-1} \tag{34}$$

3.5. Dependence of the SAW velocity vs. surface layer conductivity

Imaginary and real parts in the equations indicate changes in the attenuation and velocity of an acoustic wave [22]:

$$\frac{\Delta\alpha}{k_0} = \mathrm{Im}\left\{\frac{\Delta k}{k_0}\right\} \qquad \frac{\Delta v}{v_0} = -\mathrm{Re}\left\{\frac{\Delta k}{k_0}\right\} \tag{35}$$

When the diffusion effect vanishes (D=0), the perturbation of velocity will be independent of the frequency of the propagated wave.

The reduction of the velocity of propagation is mainly caused by two phenomena [22,30]:

a. The mass load on the crystal surface, resulting this time from the phenomenon of adsorption of gas particles on the layer surface, the surface density may be disturbed due to the additional mass of absorbed gas particles and the elastic modulus of the isotropic layer and
b. The electric "load" resulting from the interaction of the electric potential associated with the surface wave with mobile charge carriers in the layer. This results of changes in the electric conductivity of the layer due to the interaction of this chemically active layer with gas.

The electric effect has one very interesting feature, namely it causes significant changes in the propagation velocity of the SAW only in some particular range, which depends only on the properties of the piezoelectric substrate (which was $LiNbO_3$, Y-Z); the metal layer shortens the electric field associated with the surface wave [22,30]. According to this theory we can prove that surface conductivity influences the detection features of SAW gas sensors. The initial value of the conductivity determines the point of sensor work. The value of acoustoelectric interaction in the sensor configurations fulfill an important role in the sensitivity of the sensor. **Figure** 20 presents the characteristics of the relative change of a surface acoustic wave and its attenuation in the function of conductivity. In the case of $LiNbO_3$ the cuts Y-Z as piezoelectric substrate the high sensitivity range of the sensor in the region:

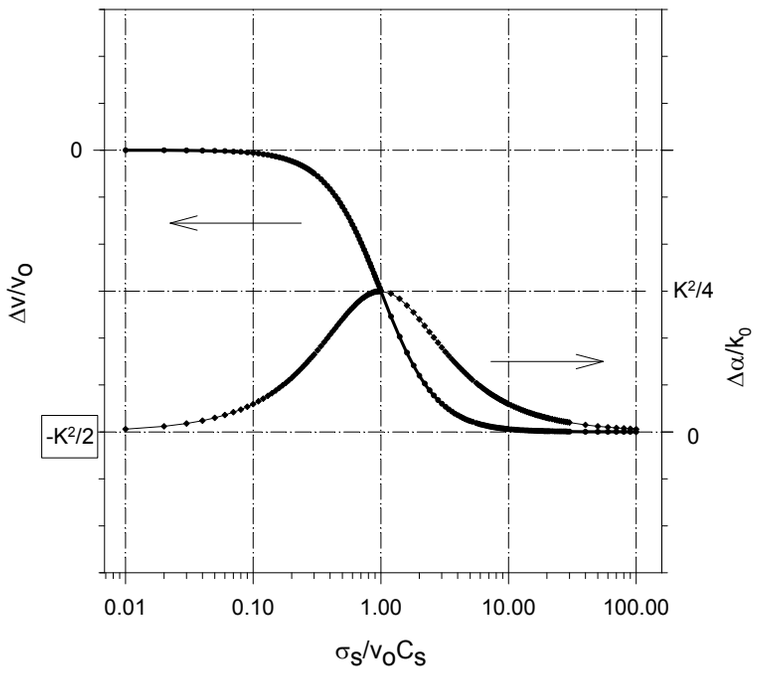

Figure 20. Velocity and attenuation of the SAW wave propagation versus the electrical conductivity of the sensor layer [22]

$$0.15 < \frac{\sigma_s}{v_0 C_s} < 5 \tag{36}$$

3.6. Analytical model of the SAW gas sensor

The concentration profile of the gas molecules in the sensor layer depends on the phenomena of gas diffusion in porous material. The mechanism of gas diffusion through a porous material depends on the size of the pores and the type of surface diffusion: Knudsen's diffusion and a molecular one. If the pores ranging from 1 to 100 nm in radius the Knudsen diffusion occurs. The Knudsen diffusion constant, D_K, depends on the molecular weight of the diffusing gas, M, the pore radius, r, temperature, T, and the universal gas constant, R, as follows [26,28]:

$$D_K = \frac{4r}{3}\sqrt{\frac{2RT}{\pi M}} \tag{37}$$

Two assumptions, i.e. Knudsen diffusion and first-order surface reaction, allow to formulate the well-known diffusion equation [26-28]:

$$\frac{\partial C_A}{\partial t} = D_K \frac{\partial^2 C_A}{\partial x^2} - kC_A \tag{38}$$

where C_A – is the concentration of target gas, t - time, y distance from the bottom layer, counted from the piezoelectric substrate, k is the rate constant.

The general solution of this equation in the steady–state condition $\frac{\partial C_A}{\partial t} = 0$ is:

$$C_A = C_1 \exp\left(y\sqrt{\frac{k}{D_K}}\right) + C_2 \exp\left(-y\sqrt{\frac{k}{D_K}}\right) \tag{39}$$

here C_1 and C_2 are integral constants.

For boundary conditions at the surface ($y = -h$): $C_A = C_{A,s}$ and $\partial C/\partial y = 0$ the following equation can be obtained [26,28]:

$$C_A = C_{A,S} \frac{\cosh(|y|\sqrt{k/D_k})}{\cosh(|-h|\sqrt{k/D_k})} \tag{40}$$

$C_{A,s}$ is the target gas concentration outside the film at the surface $y = -h$. The concentration profile depends on the thickness of the sensor layer and the constants k and D_K. The gas concentration inside the film is not constant. As in resistance sensors of the gas we may assume that the electrical conductance $\sigma(y)$ of the sheet exposed to the target gas is linear

to the gas concentration (C_A) [26]: $\sigma(y)=\sigma_0(1\pm a\cdot C_A)$, where σ_0 is the layer conductance in the air, a is the sensitivity coefficient. In resistance sensors the electrical conductance of the whole film is given by integrating $\sigma(y)$ over the whole range of y ($y = -h; -0$). That treatment has been proposed by Sakai, Williams and Hilger [26,56]. We can't treat a semiconductor layer in a homogeneous way of thinking, because the profile of molecule gas concentration in a semiconducting sensor layer changes with the distance from the piezoelectric substrate and may influence the acoustoelectric interaction differently. To analyze such a sensor layer in SAW configuration we have to assume that the film is a uniform stack of infinitesimally thin sheets with a variable concentration of gas molecules and with a different electric conductance. Each sublayer is in another distance from the piezoelectric wave-guide (**Figure** 21).

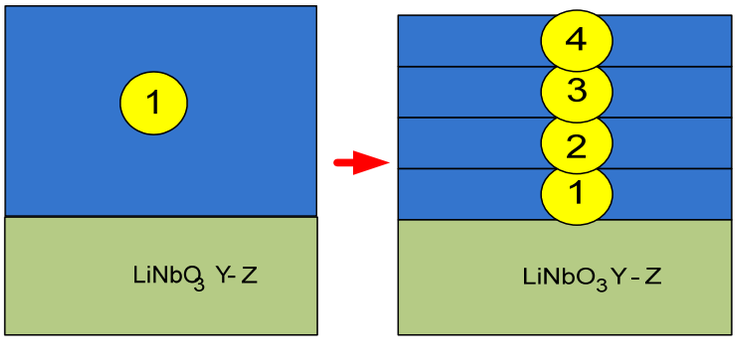

Figure 21. Model of a sensor layer in SAW system (n-sublayers) [57]

Figure 22 presents blocks whose common admittance is calculated basing on the law of impedance transformation and electronic equations. Then we applied the common impedance to the Ingebrigtsen formula.

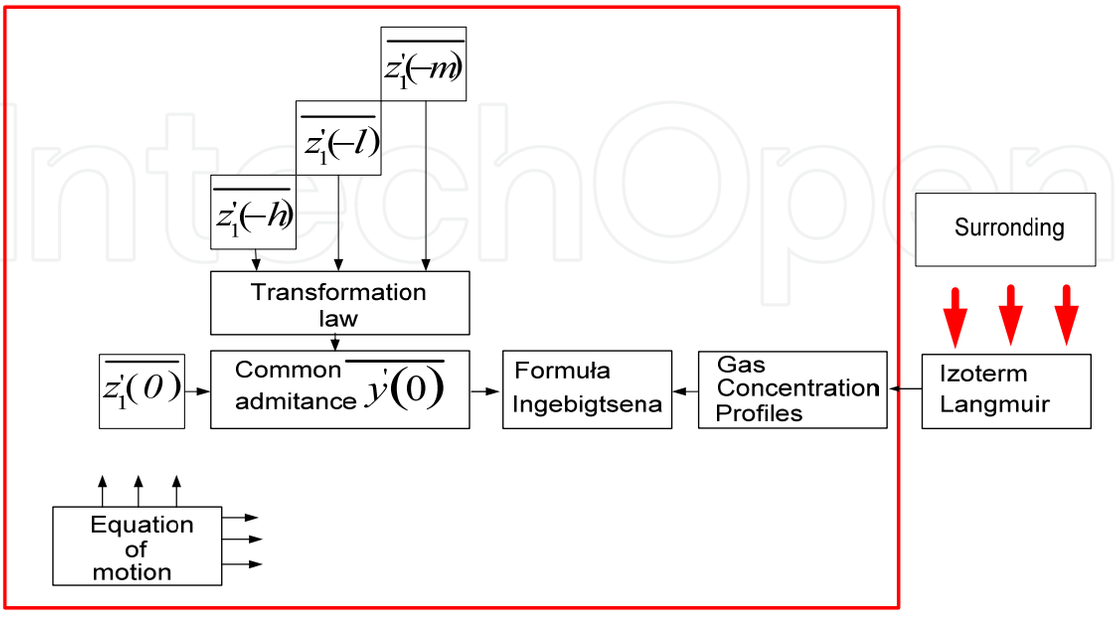

Figure 22. Diagram analysis of saw-type sensor [57]

The common admittance was applied in compliance with the Ingebrigtsen formula, which consisted in the defined impedance $z_E^{'}(0)$ on the surface at $y = 0$. The main problem was the calculation of the common normalized admittance which can be easy apply in the Ingebrigtsen formula. By using the impedance transformation law we counted the common admittance "which is seen" by an acoustoelectric wave on the plane $y = 0$.

We can see, that impedance transformation law takes the form [57]:

$$z_E^{'}(0) = \frac{i \cdot tgh\left(k_0 h\right) + z_E^{'}(-h)}{1 - i \cdot z_E^{'}(-h) \cdot tgh\left(k_0 h\right)} \tag{41}$$

The Ingebrigtsen formula for „n" sublayers is as follows [57]:

$$\frac{\Delta v}{v_0} = -\mathrm{Re}\left\{\frac{\Delta k}{k_0}\right\} = -\frac{K^2}{2} \frac{\left[\sigma_{T_2}(1 + aC_{A,y=0}) + \sum_{i=1}^{n-1} \sigma_{T_2}(y_i) f(y_i, \sigma_{T_2}(y_i))\right]^2}{\left[\sigma_{T_2}(1 + aC_{A,y=0}) + \sum_{i=1}^{n-1} \sigma_{T_2}(y_i) f(y_i, \sigma_{T_2}(y_i))\right]^2 + \left[1 + \sum_{i=1}^{n-1} g(y_i, \sigma_{T_2}(y_i))\right]^2 \left(v_0 C_S\right)^2}. \tag{42}$$

where: $C_S = \varepsilon_0 + \varepsilon_p^T$

$$f\left(y_i, \sigma\left(y_i\right)\right) = \frac{1 - \left[\mathrm{tgh}\left(k y_i\right)\right]^2}{\left[1 + \mathrm{tgh}(k y_i)\right]^2 + \left[\mathrm{tgh}(k y_i) \cdot \frac{\sigma\left(y_i\right)}{\varepsilon_0 v_0}\right]^2} \tag{43}$$

$$g\left(y_i, \sigma\left(y_i\right)\right) = \frac{\left[1 + \mathrm{tgh}(k y_i)\right]^2 + \mathrm{tgh}\left(k y_i\right) \cdot \left(\frac{\sigma\left(y_i\right)}{\varepsilon_0 v_0}\right)^2}{\left[1 + \mathrm{tgh}(k y_i)\right]^2 + \left[\mathrm{tgh}(k y_i) \cdot \frac{\sigma\left(y_i\right)}{\varepsilon_0 v_0}\right]^2} \tag{44}$$

and $\sigma_{T_2} = \sigma_{T_1} \exp\left(\frac{E_g}{2k_B} \cdot \frac{T_2 - T_1}{T_1 T_2}\right)$, $\sigma\left(y_i\right) = \sigma_0\left[1 + a \cdot C_A\left(y_i\right)\right]$, $\sigma_s = \sigma\left(0\right)$, k_B – Boltzman constant, E_g – band gap energy

3.7. Numerical results

According to the transformation law we calculated the common admittance on the surface y=0. The gas concentration profile was counted basing on the concentration of the profiles [58], which are different for gases, depending on Knudsen diffusion constants, temperature,

molecular weight, the gas constants R and the thickness of the porous sensing materials with an assumed porous radius. A simple model of a structure consisting of porous sensing material is shown in **Figure** 19. Molecular hydrogen dissociated to atomic hydrogen on the outer catalytic surface of Pd. Adsorbed hydrogen atoms then act as electrical dipoles at the metal semiconductor interface and involve changes in the work function in the surface conductivity of the semiconductor material [53,58]. The target gas, diffusing in the sensing layer, is gradually consumed in the surface reaction. Under steady-state conditions the gas concentration inside the sensing layer decreases with the increasing diffusion depth, resulting in a gas concentration profile which depends on the rates of the surface reaction and diffusion reaction. Other gases like NH_3, CO_2, NO_2 can diffuse similarly as hydrogen into porous sensing material depending on its temperature, molecular weight and the physical parameters of the sensing layers.

Some numerical results concerning the gases mentioned above are presented in **Figures** 23, 24, 25. We assume the following values for the involved constant $\sigma_s = v_0 C_S = 1.6x10^{-8}[\Omega^{-1}]$, sensitivity coefficient a=1 [ppm^{-1}], thickness of the sensor layer 100 [nm], temperature 300 [K], pore radius 5 [nm]. As a sensor layer we use thin film of WO_3.

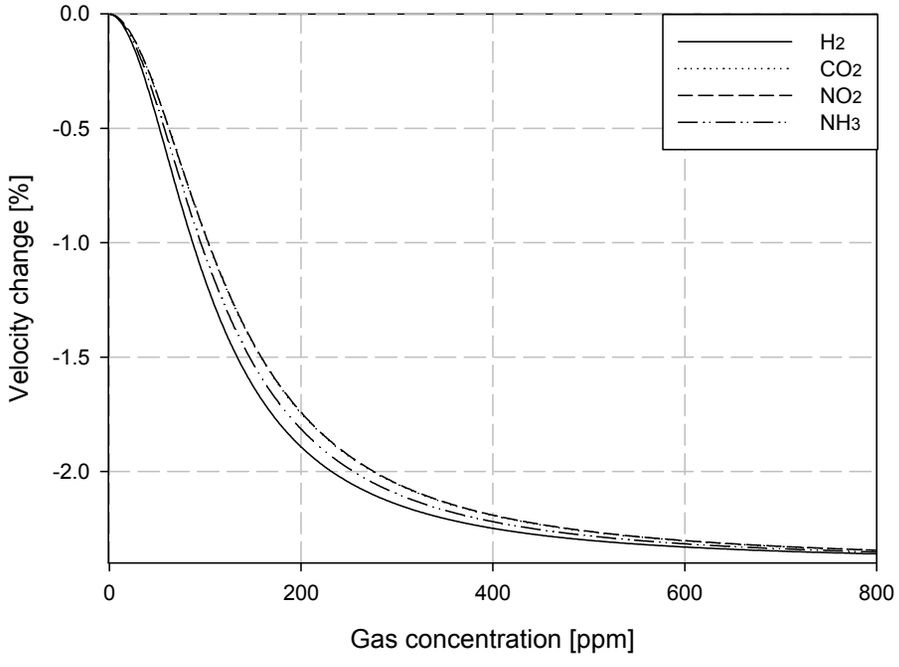

Figure 23. Velocity changes of the SAW wave propagation vs. gas concentration [58]

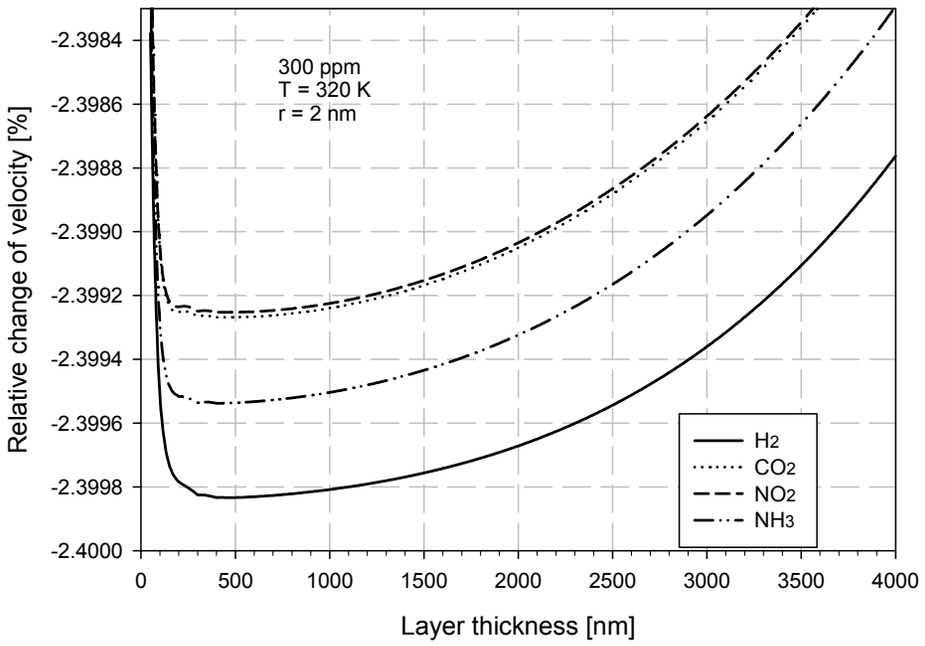

Figure 24. SAW wave propagation velocity changes vs. thickness of the sensor layer for 300 ppm H_2, CO_2, NO_2 or NH_3 [58]

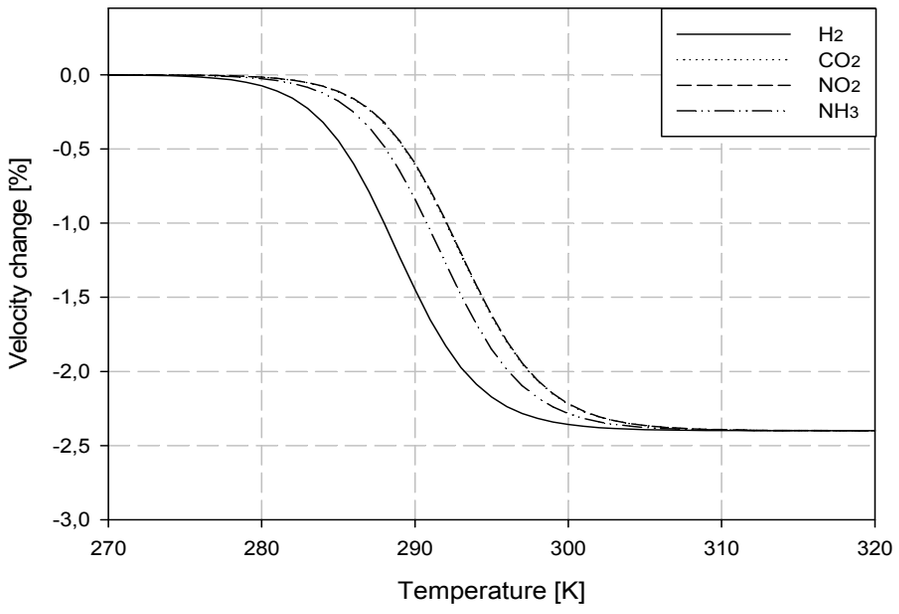

Figure 25. SAW wave propagation velocity changes vs. temperature of the sensor layer [58]

3.8. Conclusions

a. Experimental studies have shown high sensitivity dual sensor layer system especially: semiconducting polymer layer (CuPc) and palladium catalyst thin layer for hydrogen detection. It is also observed in the palladium phase transition at concentrations above 2% hydrogen in synthetic air.

b. The designed mathematical model of a SAW sensor is based on the electric effect which results from changes in the electric surface conductivity of the layers $\sigma_s(y)$, due to the interaction of this chemically active layer with gas.
c. In the analytical model we introduce sheet conductance which is assumed to be linear to the gas concentration.
d. We divided the porous semiconductor layer into sublayers. According to the transformation law we calculated the influence of the impedance above the piezoelectric substrate on the relative change of velocity versus the concentration, thickness, size of the pores and temperature.
e. We assumed the Knudsen diffusion in porous sensing materials in which pores in the range from 1 to 100 nm in radius do prevail.
f. The analytical model allows the optimization of sensor parameters of a sensor layer and the correct choice of sensor conditions

Author details

Marian Urbańczyk and Tadeusz Pustelny
Silesian Univ. of Technology, Faculty of Electrical Engineering, Department of Optoelectronics, Gliwice, Poland

Acknowledgement

This work is financed as a grant of the National Center of Research and Development PBR OR 00017912.

4. References

[1] Pieka A (2002) Physics of Surface Semiconductor, IUU, Kijev.
[2] Kittel C (2006) Introduction to solid state physics, John Wiley & Sons, Amsterdam.
[3] Ziman J.M (1996) Principles of the theory of solids, Cambridge Press.
[4] Calloway J (1997) Quantum theory of the solid state, Academic Press, Berlin.
[5] Deleven R. (1990) Introduction to applied state physics, Plenum, Roma.
[6] Seitz F (2008) Solid state physics, advances in research and applications, Academic Press, Berlin.
[7] Sliwinski A. (2001) Ultrasounds and their application, WNT, Warsaw.
[8] Gulayev Y (2000) On the nonlinear theory of ultrasound application in semiconductors, Phys. Usp. 48(8): 847-855.
[9] Das P (2006) Method for providing in-situ non-destructive monitoring of semiconductor surface, Molecular and Quantum Acoustics, vol. 26, No 11, 87-89
[10] Taguchi N (1971) Gas detecting device, US Patent, 3,631,436.
[11] Lundstrom I, Sodeberg D (1981/1982) Hydrogen sensitive MOS structures, part 2: characterization, Sensors and Actuators 2: 105-117.

[12] Mizsei J, Lantto V (1992) Air pollution monitoring with a semiconductor gas sensor array system, Sensors and Actuators B6:223-229.
[13] Comini E, Guidi V, Frigeri C, Ricco I, Sberveglieri G (2001) CO sensing properties of titanium and iron nanosized thin films, Sensors and Actuators B, vol.77:6-21.
[14] Bai Hua, Shi Gaoquan (2007) Gas sensors based on conducting polymers, Sensors vol.7:267-307.
[15] Adhikari B, Majumdar S (2004) Polymers in sensor applications, Prog. Polym. Scie. Vol.29:669-766.
[16] Harsanyi G (1995) Polymer films in sensor applications, Technomic, Budapest, Basel.
[17] Janata J, Huber R. (1985) Solid state chemical sensors, Academic Press, INC.
[18] D'Amico A, Verona E (1989), SAW sensors, Sensors and Actuators, 17:55-66.
[19] Maciak E, Opilski Z, Urbańczyk M (2005) Pd/V_2O_5 fiber optic hydrogen gas sensor, J.de Phys. IV France 129:137-141.
[20] Ignac-Nowicka J, Pustelny T, Opilski Z, Maciak, Jakubik W, Urbańczyk M (2003) Examination of thin films of phthalocyanines in plasmon system for application In NO_2 sensors, Opt. Eng. 42(10): 2978-2986.
[21] Thompson M, Stone D (1997) Surface-Launched Acoustic Wave Sensors. Chemical Sensing and Thin-Film characterization. Chemical analysis vol.144, J Willey and Sons.
[22] Jakubik W, Urbanczyk M (1997) The electrical and mass effect in gas sensors of the SAW type J. Tech. Phys. IV 38: 589-595.
[23] Auld B (1973) Acoustic Fields and Waves, vol. 1, 2 John Willey and Sons, New York.
[24] Jakubik W, Urbańczyk M, Kochowski S, Bodzenta J (2002) Bilayer structure for hydrogen detection in a surface acoustic wave sensor system, Sensors and Actuators B, 82:265-271.
[25] Jakubik W (2006), Investigations of bilayer sensor structure with copper phthalocyanine and palladium for hydrogen detection in SAW system, Journal de Physique IV, vol.137: .95-98.
[26] Sakai Go, Matsunaga Naoki, Shimanoe Engo, Yamazone Noboru (2001), Theory of gas-diffusion controlled sensitivity for thin film semiconductor gas sensor, Sensors and Actuators B 80:125-131.
[27] Gardner J W (1990), A non – linear diffusion – reaction model of electrical conduction in semiconductor gas sensors, Sensors and Actuators, B1:166-170.
[28] Pisarkiewicz T (2007), Mikrosensory gazów, AGH Kraków, Poland.
[29] Ingebrigtsen K A (1970), Linear and nonlinear attenuation of Acoustic Surface Waves in a Piezoelectric Coated with a semiconducting film, J.Appl.Phys. vol.41, No 2:454-459.
[30] Hejczyk T, Urbańczyk M, Jakubik W (2010) Semiconductor Sensor Layer in SAW Gas Sensors Configuration, Acta Physica Polonica A, vol. 118: 1152-1156.

[31] Adler R., Datta S (1988) Acoustoelectric Mobility Measurements on Films with Negligible Acoustic Loss, IEEE SU, 10: 139-144.
[32] Tabib-Azar M (1988) Characterization of Electrical Properties of Semi-Insulating GaAs Using Acousto-Electric Voltage Spectroscopy, Solid-State Electronics, v.31, 7:1197-1204.
[33] Pustelny T, Opilski A (1989) Investigations Concerning Fast Surface States of Semiconductors by Means of Acoustic Methods, Archives of Acoustics, 14, 3:253-260.
[34] Pustelny T, Kubik Z (1993) Acoustic Methods of the Determination of Surface Potential in GaAs, Molecular and Quantum Acoustic,. 14:112-120.
[35] Pustelny T, Kubik Z (1994) Investigation of Surface Potential of GaAs Surface by Means of Acoustics Effects, Archives Acoustics, 19, 2:271-280.
[36] Hoskins M.J. Morkov V. (1982) Charge transport by surface acoustic wave in GaAs, Appl. Phys. Lett., vol. 41:332-343.
[37] Barbe D.F. (1986) Charge-Coupled sefices, Topics Appl. Phys., vol. 38, Springer, Berlin, Heidelberg.
[38] Kino G.S. (1987) Acoustic Waves; Devices, Imaging and Analog Signal Processing, Prentice Hall. Englewood Cliffs, New York.
[39] Parker T.E., Monterss G.K (1988) precision surface acoustic wave (SAW) oscillators. IEEE Trans. on Ultrasonics, Ferroelectroics and Frequency Control, 35:342-364.
[40] Melen R, Buss D, (1999) Charge coupled Devices: Technology and Applications, Wiley & Sons, New York.
[41] Howes M.J, Morgan D.V (1991) Charge coupled devices and systems, Wiley & Sons, New York.
[42] Pustelny T, Pustelna B (2006) The acoustic method of investigating the electrical carrier mobilituy of the real GaP:Te (100) surface, Journal de Physique IV, 137:223-226.
[43] Gulajew J.W (1985) Issledovanije nieliniejnych akustoelektriczeskich effektow i akustoprowodimosti w sloistoj strukturie piezoelektrik- poluprowodnik, Fiz. Twiord. Tiela, 17, 12:3505-3513.
[44] Pustelny T, Pustelny B (2008) The acoustic method of the surface potential investigation in GaP:Te (110) real surface, European Physical Journal: Special Topics,Volume 154, Issue 1: 281-284.
[45] Pustelny T, Adamowicz B (1994) Transverse Acoustoelectric Effect and Surface Photovoltage Method in Surface Study of GaP and InP, J. Tech. Phys., 3:75-86.
[46] Pustelny B, Pustelny T (2009) Transverse acoustoelectric effect applying in surface study of Gap:Te(111), Acta Phys. Pol. A, 116(3):383-384.
[47] Pustelny T, Opilski A, Pustelny B, (2008) Determination of some kinetic parameters of fast surface states in silicon single crystals by means of surface acoustic wave method, Acta Phys. Pol. A, 114(6A):A183-A190.
[48] Pustelny T (1995) Acoustic method of investigating the surface potential in semiconductors. Study of the GaP:Te (110) real surface, Ultrasonics, 33(4):289-294.

[49] Pustelny T (1997) Surface Acoustic Wave Techniques for the Real-Surfaces Investigations of InP (111), InAs (111) Semiconductors, Acustica-acta acoustics, vol. 83 (3):482-488
[50] Matthews H (1997) Surface wave filters Design, construction and use, J Wiley and Sons, New York.
[51] D'Amico A, Palma A, Verona E (1982), Hydrogen sensor using a palladium coated surface acoustic wave delay-line, IEEE Ultrasonics Symposium: 308-311.
[52] Jakubik W, Urbańczyk M, Kochowski S, Nadolski M (2001) Surface acoustic wave sensor for hydrogen detection with a two-layered structure, Molecular and Quantum Acoustics, vol. 22: 123-131.
[53] Jakubik W (2007), Investigation of thin film structure of WO_3 and WO_3 with Pd for hydrogen detection in a surface acoustic wave sensor system, Thin Solid Films, 515: 8345-8350
[54] Tiersten H, Sinha B.K (1978) A perturbation analysis of the attenuation and dispersion of surface waves, J. Appl. Phys., vol. 49, No. 1.
[55] White R (1970), Surface elastic waves, Proc. IEEE, vol.58, No8:1238-1277.
[56] Williams D E, Hilger A, (1987), Solid state gas sensors, Bristol and Philadelphia.
[57] Hejczyk T, Urbańczyk M, Jakubik W (2010), Analytical Model of Semiconductor Sensor Layers in SAW Gas Sensors, Acta Physica Polonica A, vol 118:1148-1152.
[58] Hejczyk T, Urbańczyk M, Jakubik W (2010), Numerical Results of Modeling Semiconductor Sensor Layers in SAW Gas Sensors, Acta Physica Polonica A, vol 118:1157-1159.